NRL Memorandum Report 4670

Formulation of Normalized Non-Linear Free Electron Laser Equations

C. M. TANG AND P. SPRANGLE

Plasma Theory Branch
Plasma Physics Division

December 9, 1981

This work was supported by the Defense Advanced Research Projects Agency
under Contract No. 3817.

NAVAL RESEARCH LABORATORY
Washington, D.C.

SECURITY CLASSIFICATION OF THIS PAGE (When Data Entered)

REPORT DOCUMENTATION PAGE	READ INSTRUCTIONS BEFORE COMPLETING FORM
1. REPORT NUMBER: NRL Memorandum Report 4670	2. GOVT ACCESSION NO.: AD-A108358
	3. RECIPIENT'S CATALOG NUMBER
4. TITLE (and Subtitle): FORMULATION OF NORMALIZED NON-LINEAR FREE ELECTRON LASER EQUATIONS	5. TYPE OF REPORT & PERIOD COVERED: Interim report on a continuing NRL problem.
	6. PERFORMING ORG. REPORT NUMBER
7. AUTHOR(s): C.M. Tang and P. Sprangle	8. CONTRACT OR GRANT NUMBER(s)
9. PERFORMING ORGANIZATION NAME AND ADDRESS: Naval Research Laboratory, Washington, DC 20375	10. PROGRAM ELEMENT, PROJECT, TASK AREA & WORK UNIT NUMBERS: 62310E; ARPA No. 3817; 47-0867-01
11. CONTROLLING OFFICE NAME AND ADDRESS	12. REPORT DATE: December 9, 1981
	13. NUMBER OF PAGES: 42
14. MONITORING AGENCY NAME & ADDRESS(if different from Controlling Office)	15. SECURITY CLASS. (of this report): UNCLASSIFIED
	15a. DECLASSIFICATION/DOWNGRADING SCHEDULE

16. DISTRIBUTION STATEMENT (of this Report)

Approved for public release; distribution unlimited.

17. DISTRIBUTION STATEMENT (of the abstract entered in Block 20, if different from Report)

18. SUPPLEMENTARY NOTES

19. KEY WORDS (Continue on reverse side if necessary and identify by block number)

Free electron laser

20. ABSTRACT (Continue on reverse side if necessary and identify by block number)

The general non-linear self-consistent equations describing the FEL in the steady state amplifying configuration is derived with the space charge effects and all the efficiency enhancement schemes: i) a spatially varying wiggler amplitude and/or period and ii) a D.C. electric field $E_{DC}(z) = [-\partial\phi_{DC}/\partial z]\hat{e}_z$. All the efficiency enhancement schemes are shown to be somewhat equivalent. For a variable period magnetic wiggler, the FEL equations can be appropriately normalized to a three parameter set of coupled equations.

(Continues)

DD FORM 1 JAN 73 1473 EDITION OF 1 NOV 65 IS OBSOLETE
S/N 0102-014-6601

SECURITY CLASSIFICATION OF THIS PAGE (When Data Entered)

20. ABSTRACT (Continued)

All operating regimes are covered by these normalized equations. The condition for space charge to be unimportant is given. In the absence of the space charge effects, the three parameter set of equations reduces to a two parameter set. The inclusion of additional efficiency enhancement schemes increases the number of parameters to describe the FEL. Curves showing the efficiency, radiation amplitude and growth rate will be presented.

CONTENTS

FORMULATION OF NORMALIZED NON-LINEAR FREE ELECTRON LASER EQUATIONS

I. Introduction

Free electron lasers (FELs) show great potential for becoming a new class of efficient devices capable of generating intense levels of coherent radiation, continuously tunable from sub-millimeter to beyond the optical regime.[1-35] The FEL is characterized by a wiggler (pump) field, for example a spatially periodic magnetic field, which scatters off a relativistic electron beam.

In this paper we present an extension of the formulation of the 1-D non-linear self-consistent FEL equations in the steady state amplifying configuration with space charge effect for a circularly polarized wiggler field.[26,27,31] We included all the efficiency enhancement schemes: i) a spatially varying wiggler amplitude and period[26-28,31] and ii) a D.C. electric field $E_{DC}(z) = -\left[\partial\phi_{DC}/\partial z\right]\hat{e}_z$.[32-35] We show that all the efficiency enhancement schemes are somewhat equivalent. The complete FEL equations cover all operating regimes.

For a variable period magnetic wiggler field, the FEL equations can be appropriately normalized to contain only three parameters. All operating regimes are covered by the three parameters. The condition for space charge to be neglected is derived. In the absence of the space charge effects, the three parameter set of equations is reduced to a two parameter set.

In the high gain regime, we present graphs of growth rate, efficiency and saturation amplitudes of the radiation field.

In the low gain regime, we obtained the linear gain expression

Manuscript submitted September 9, 1981.

with the space charge effect.[27,37,38] We give an example of a FEL experiment where space charge effect is somewhat important. We compared results of linear theory with results from non-linear calculations.

II. Normalized FEL Equations with Space Charge Effects

We present a self-consistent non-linear theory of the FEL in the steady state amplifying configuration, see Fig. (1). Included in our analysis are space charge effects and the following efficiency enhancement schemes: i) contouring, spatially, the amplitude and/or the wavelength of the magnetic wiggler field, and ii) by applying an external D.C. electric field, $\underset{\sim}{E}_{DC} = -\frac{\partial \phi_{DC}}{\partial z}\hat{e}_z$.

The right handed circularly polarized external magnetic wiggler field in terms of the vector potential is

$$\underset{\sim}{A}_0(z) = A_0(z)(\cos(\int_0^z k_0(z')dz')\hat{e}_x+\sin(\int_0^z k_0(z')dz')\hat{e}_y) \quad , \tag{1}$$

where $k_0(z)$ is the spatially varying wiggler wavenumber. The vector and scalar potential corresponding to the radiation and space charge field are represented by

$$\underset{\sim}{A}(z,t) = A(z)(\cos(\int_0^z k_+(z')dz' - \omega t)\hat{e}_x-\sin(\int_0^z k_+(z')dz' - \omega t)\hat{e}_y) \, , \tag{2a}$$

$$\begin{aligned}\phi(z,t) = {} & \phi_1(z)\cos(\int_0^z (k_+(z')+k_0(z'))dz' - \omega t) \\ & +\phi_2(z)\sin(\int_0^z (k_+(z')+k_0(z'))dz' - \omega t) \, ,\end{aligned} \tag{2b}$$

where $A(z)$, $\phi_1(z)$, $\phi_2(z)$ and $k_+(z)$ are the spatially slowly varying amplitudes and wavenumber of the fields. The frequency ω of the radiation and space charge wave is taken to be constant.

Equations governing the spatial evolution of the potentials $A(z,t)$ and $\phi(z,t)$ have been derived elsewhere.[26-27] We begin our analysis with the fully non-linear, self-consistent equations for $A(z)$, $k_+(z)$, $\phi_1(z)$ and $\phi_2(z)$:

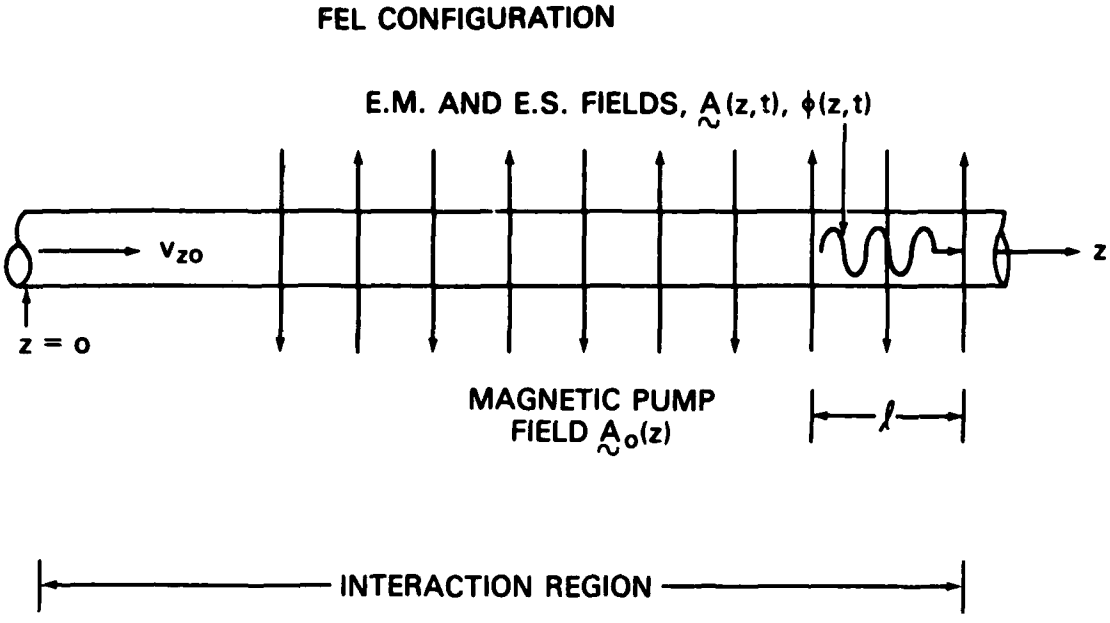

Fig. 1 — Schematic of the Free Electron Laser model. The unmodulated electron beam enters the interaction region from the left. In this figure the wiggler (pump) field builds up adiabatically and reaches a constant amplitude and wavelength for $z > 0$. The pump field may in general have a varying period and amplitude, which is not shown in this figure.

$$(\omega^2/c^2 - k_+^2(z))A(z) = F_{em}\frac{\omega_b^2}{2c^2} m_0 v_{zo} \frac{\omega}{\pi}\int_0^{2\pi/\omega} \frac{dt_0}{p_z(z, t_0)}$$

$$\left\{A_0(z)\cos\psi(z,t_0) + A(z)\right\} , \tag{3a}$$

$$2k_+^{\frac{1}{2}}(z)\frac{\partial}{\partial z}(A(z)k_+^{\frac{1}{2}}(z)) = - F_{em}\frac{\omega_b^2}{2c^2} m_0 v_{zo} \frac{\omega}{\pi}\int_0^{2\pi/\omega} \frac{dt_0}{p_z(z, t_0)}$$

$$\left\{A_0(z)\sin\psi(z,t_0)\right\} , \tag{3b}$$

$$(k_+(z) + k_0(z))\phi_1(z) = - F_{sc}\frac{\omega_b^2}{c^2}\frac{m_0c^2}{|e|}\frac{v_{z0}}{\pi}\int_0^{2\pi/\omega} dt_0\cos\psi(z, t_0) , \tag{3c}$$

$$(k_+(z) + k_0(z))\phi_2(z) = - F_{sc}\frac{\omega_b^2}{c^2}\frac{m_0c^2}{|e|}\frac{v_{z0}}{\pi}\int_0^{2\pi/\omega} dt_0 \sin\psi(z, t_0) , \tag{3d}$$

$$\psi(z, t_0) = \int_0^z (k_+(z') + k_0(z') - \omega/v_z(z', t_0))dz' - \omega t_0 , \tag{4}$$

where $\omega_b = (4\pi|e|^2 n_0/m_0)^{\frac{1}{2}}$, n_0 is the local beam density, F_{em} is the filling factor for the electromagnetic field, F_{sc} is the filling factor associated with the space charge field, v_{z0} is the initial axial beam velocity, $v_z(z,t_0)$ is the axial velocity at position z of a particle which was at z = 0 at time t_0, $p_z(z,t_0) = \gamma(z,t_0)m_0v_z(z,t_0)$ is the corresponding axial particle momentum and

$$\gamma(z,t_0) = (1 + |e|^2(\underset{\sim}{A}_0(z) + \underset{\sim}{A}(z,\tau))^2/m_0^2c^4 + p_z^2(z,t_0)/m_0^2c^2)^{\frac{1}{2}} , \tag{5}$$

where $\tau(z,t_0) = \int_0^z v_z(z', t_0)dz' + t_0$, is the time it takes a particle to reach the position z if it entered the interaction region z=0 at time t_0. The phenomenological filling factors, F_{em} and F_{sc} are less than unity and in general not equal. Roughly speaking, F_{em} is the ratio of the cross

sectional area of the electron beam to the effective area of the radiation beam. Since the radiation field is not directly supported by the electron beam, F_{em} can be much less than unity. The space charge field, on the other hand, propagates on the electron beam and falls off rapidly away from the beam. Hence F_{sc} can be close to unity. For a fixed electron beam radius, F_{em} decreases as the radiation, beam radius increases while F_{sc} approaches unity as the radius of the cylindrical waveguide containing the electron beam increases. Physically, the reduced beam plasma frequency $F_{sc}\,\omega_b$ is less than the local plasma frequency ω_b. The parameter F_{sc} can also be referred to as the plasma frequency reduction factor. In the usual case, where F_{em} is much less than unity, the space charge wave filling factor is close to unity, $F_{sc} \approx 1$, Chapter 8 of Ref. (31).

Note that in Eqs. (3) the electron beam has been assumed to be initially mono-energetic. Generalization to an initially thermal beam is straightforward and considered in a previous one-dimensional formulation of this problem.

The integrands in Eqs. (3) contain the particle dynamics which are determined from the Lorentz force equations. It is straightforward to show that the axial particle velocity $v_z(z,t_0)$, expressed in terms of the independent variables z and t_0, satisfies

$$\frac{d\,v_z(z,t_0)}{dz} = \frac{|e|^2}{m_0^2\,c^3}\,\frac{1}{\gamma_{\perp 0}^2\,\gamma_z^2(z,t_0)}\left[-\tfrac{1}{2}\frac{\partial\,A_0^2(z)}{\partial z} - \frac{\partial A_0(z)A(z)}{\partial z}\cos\psi(z,t_0)\right.$$
$$+A_0(z)A(z)\left(k_+(z) + k_0(z) - \frac{v_z(z,t_0)}{c}\,\frac{\omega}{c}\right)\sin\psi(z,t_0)$$
$$-\frac{\gamma_{\perp 0}}{\gamma_z(z,t_0)}\frac{m_0c^2}{|e|}\,(k_+(z) + k_0(z))(\phi_1(z)\sin\psi(z,t_0)$$
$$\left.-\phi_2(z)\cos\psi(z,t_0))\right] + \frac{|e|}{m_0\gamma_{0\perp}\gamma_z^3(z,t_0)c}\,\frac{\partial\phi_{DC}}{\partial z}\,, \qquad (6)$$

where $\gamma_{\perp 0} = (1 + (|e|A_0/m_0c^2)^2)^{\frac{1}{2}}$, $\gamma_z(z, t_0) = (1 - v_z^2(z, t_0)/c^2)^{-\frac{1}{2}}$ and $\gamma(z,t_0) = \gamma_{\perp 0}\gamma_z(z,t_0)$.

From (6) we can derive an equation for the phase $\psi(z, t_0)$. We first define $v_z(z, t_0) = v_{z0} + \delta v_z(z, t_0)$, $\Delta k(z) = (k_+(z) + k_0(z) - \omega/v_{z0})$ and $\omega = \omega_0 + \Delta\omega$ where $|\delta v_z| << v_{z0}$, $\omega_0 = (1+\beta_{z0})\ \gamma_{z0}^2 v_{z0} k_0(0)$ and $|\Delta\omega| << \omega_0$. Noting that $\delta v_z(z, t_0) \approx v_{z0}^2\ (\partial\psi(z,t_0)/\partial z - \Delta k(z))/\omega$ and $k_+(z) + k_0(z) - v_z(z, t_0)\omega/c^2 \approx 2k_0(0)(1 + \Delta k(z)/k_0(0) - (2k_0(0))^{-1}\partial\psi(z, t_0)/\partial z)$ we find that Eq. (6) takes the form

$$\frac{\partial^2\psi(z, t_0)}{\partial z^2} = \frac{\partial\Delta k(z)}{\partial z} - \frac{2|e|^2}{m_0^2 c^4}\ \frac{k_0(0)}{\gamma_{\perp 0}^2 h^2(z, t_0)}\ \frac{d A_0^2(z)}{dz}$$

$$+ \frac{|e|\gamma_{0\perp}{}^2\ \omega/c^3}{m_0\gamma_0{}^3 h^3(z, t_0)}\ \frac{d\phi_{DC}}{dz} + \frac{4|e|^2}{m_0^2c^4}\ \frac{k_0^2(0)}{\gamma_{\perp 0}^2 h^2(z, t_0)}$$

$$\left[A_0(z)A(z)\left(\frac{1}{h^2(z, t_0)} + \frac{1}{2k_0(0)}\ \frac{\partial\psi(z,t_0)}{\partial z}\right)\sin\psi(z, t_0)\right.$$

$$\left. - \frac{\gamma_0}{h(z,t_0)}\ \frac{m_0c^2}{|e|}\ (\phi_1(z)\ \sin\psi(z, t_0) - \phi_2(z)\ \cos\psi(z, t_0))\right], \quad (7)$$

where $$h(z,t_0) = \gamma_z(z, t_0)/\gamma_{z0} = \left[1 - k_0^{-1}(0)\ \frac{\partial\psi(z,t_0)}{\partial z} + \frac{\Delta k(z)}{k_0(0)}\right]^{-\frac{1}{2}}.$$

In obtaining (7) we have made the added assumptions that A(z) changes little over a wiggler period. The various efficiency enhancement schemes ((1) contouring the wiggler period, (2) contouring the wiggler amplitude and, (3) application of a D.C. electric potential) are represented by the first three terms of Eq. (7) respectively. The affect of the various schemes on the phase are equivalent.

In the following, we will consider a simplified example where the D.C. electric field is zero, $E_{DC} = \frac{d\phi_{DC}}{dz} = 0$, the amplitude of the magnetic wiggler A_o is constant, and $k_o(z) = k_o(0)(1 + \varepsilon(z))$. We will show that the FEL equations can be normalized in such a way as to be functions of only three parameters, and to be functions of only two parameters in the absence of space charge-effects. For $\gamma_0 >> 1$, the complete set of coupled equations in (3) and (7) can be written as

$$\frac{\partial^2 \psi(\tilde{z}, \tilde{t}_0)}{\partial \tilde{z}^2} = \frac{d\delta k(\tilde{z})}{d\tilde{z}} + \frac{C_0^2 a(z)}{h^2(\tilde{z}, \tilde{t}_0)}\left[h^{-2}(\tilde{z}, \tilde{t}_0) + \frac{1}{2}\frac{\partial\psi(\tilde{z},\tilde{t}_0)}{\partial\tilde{z}}\right]\sin\psi(\tilde{z},\tilde{t}_0)$$

$$\frac{+2\pi D_0^2}{h^3(\tilde{z}, \tilde{t}_0)}\left[\langle\cos\psi(\tilde{z},\tilde{t}_0)\rangle\sin\psi(\tilde{z}, \tilde{t}_0) - \langle\sin\psi(\tilde{z}, \tilde{t}_0)\rangle\cos\psi(\tilde{z}, \tilde{t}_0)\right], \quad (8a)$$

$$(\delta k(\tilde{z}) - \varepsilon(\tilde{z}))\, a(\tilde{z}) = -2\pi\langle h^{-1}(\tilde{z}, \tilde{t}_0)\cos\psi(\tilde{z}, \tilde{t}_0)\rangle, \quad (8b)$$

$$\frac{da(\tilde{z})}{d\tilde{z}} = -2\pi\langle h^{-1}(\tilde{z}, \tilde{t}_0)\sin\psi(\tilde{z}, \tilde{t}_0)\rangle, \quad (8c)$$

where $\tilde{z} = k_0(0)z$ is the normalized axial distance, $\tilde{t}_0 = \omega t_0$, $\delta k(\tilde{z}) = \Delta k(\tilde{z})/k_0(0) + \Delta\omega/\omega_0$, $\Delta k(\tilde{z}) = (k_+(\tilde{z}) + k_0(\tilde{z}) - \omega/v_{z_0})$, $\omega = \omega_0 + \Delta\omega$, $\omega_0 = (1+\beta_{z0})\,\gamma_{z0}^2 v_{z0} k_0(0)$, $|\Delta\omega| << \omega_0$, $h(\tilde{z}, \tilde{t}_0) = \gamma_z(\tilde{z}, \tilde{t}_0)/\gamma_{z0} = (1+\Delta k(\tilde{z})/k_0(0) - \partial\psi(\tilde{z},\tilde{t}_0)/\partial\tilde{z})^{1/2}$. $\langle(\ldots)\rangle = \int_0^{2\pi}(d\tilde{t}_0/2\pi)(\ldots)$ is the ensemble average operator $a(\tilde{z}) = 8\pi(\gamma_{z0}/\xi)^2 A(\tilde{z})/A_0$ is the normalized radiation field, $\xi = \sqrt{F_{em}}\,\omega_b/(\sqrt{\gamma_0}ck_0(0))$ is the beam strength parameter, $C_0^2 = (|e|A_0\xi/\gamma_0 m_0 c^2)^2/2\pi = \beta_{0\perp}^2\xi^2/2\pi$, $D_0^2 = (F_{sc}/F_{em})\xi^2/\pi\gamma_{z0}^2$ is the space charge parameter, $c\beta_{0\perp} = |e|A_0/\gamma_0 m_0 c$ is the transverse particle velocity due to

the magnetic pump field.

In obtaining Eq. (5) from (3) and (4) we made use of the approximations $|(A/2k_+)\ \partial k_+/\partial z| << \partial A/\partial z$, $\omega^2 - c^2k_+^2(z) \approx 2\omega(\omega - ck_+(z))$, $v_z(z,t_0) \approx v_{z0} + v_{z0}^2\ (\partial\psi(z,t_0)/\partial z - \Delta k(z))/\omega$ and where appropriate $(k_+(z) + k_0(z)) \approx \omega/c$

The space charge potential is given by

$$\phi_{1,2}(\tilde{z}) = -\frac{\pi}{2}\ \frac{m_0c^2}{|e|}\ \frac{\gamma_{\perp 0}}{\gamma_{z0}}\ D_0^2 \begin{Bmatrix} \langle\cos\psi\ (\tilde{z},\ \tilde{t}_0)\rangle \\ \langle\sin\psi\ (\tilde{z},\ \tilde{t}_0)\rangle \end{Bmatrix}, \qquad (9)$$

where $\gamma_{\perp 0} = \gamma_0/\gamma_{z0} = (1 + |e|^2A_0^2/m_0^2c^4)^{\frac{1}{2}}$.

The coupled set of normalized equations in (8) completely describe both the linear and non-linear behavior of the FEL process for a varying period magnetic pump field. These equations include the effects of space charge in both the low gain limit (interference regime) as well as the high gain limit for arbitrary magnetic pump amplitudes. Space charge effect is manifested in the last term of the modified pendulum equation, i.e., Eq. (8a). The general initial conditions needed to solve the FEL equations in (8) are simply $\delta\tilde{k}(0) = 0$, $\varepsilon(0) = 0$, $h(0,\tilde{t}_0) = 1, \psi(0,\tilde{t}_0) = -\tilde{t}_0$ and $\partial\psi(\tilde{z},\ \tilde{t}_0)/\partial\tilde{z}|_{z=0} = -\Delta\omega/\omega_0$ where $\Delta\omega = \omega - \omega_0$ is the frequency mismatch and $\omega_0 = (1 + \beta_{z0})\gamma_{z0}^2 v_{z0} k_0(0)$.

For completeness, the linear dispersion relation[24-26] can also be written in terms of the normalized variables.

$$\delta k(\delta k - \zeta_1)(\delta k - \zeta_2) = -\pi C_\eta^2(1 + \delta k) \qquad (10)$$

where

$$\zeta_1 = \frac{\Delta\omega}{\omega_0} + \frac{\pi}{4} D_0^2 + \sqrt{\pi D_0^2}\ ,$$

$$\zeta_2 \frac{\Delta\omega}{\omega_0} + \frac{\pi}{4} D_0^2 - \sqrt{\pi D_0^2}\ .$$

Im (δk) is the normalized growth rate and $L_e = (k_0(0)\ \text{Im}\ (\delta k))^{-1}$ is the e-folding length of the radiation.

Efficiency is defined as

$$\eta = \frac{\gamma_0 - \langle \gamma(\tilde{z},\tilde{t}_0)\rangle}{\gamma_0 - 1} \tag{11a}$$

For $F_{em} = F_{sc} = 1$ and $\gamma_0 >> 1$,

$$\eta \simeq \frac{C_0^2}{8\pi}\ (1 + \frac{\Delta\omega}{\omega_0})\ (\ a^2(\tilde{z}) - a^2(0))\ . \tag{11b}$$

In the absence of space charge effects we have a two parameter set of equations for both the low gain and high gain limits. In the low gain limit the two input parameters are $C_0^2\ a(0)$ and $\Delta\omega/\omega_0$ while in the high gain limit the two parameters are C_0^2 and $\Delta\omega/\omega_0$. All operating regimes of the FEL are therefore completely covered by two parameters when space charge effects can be neglected. The inclusion of space charge effects introduces a third parameter D_0^2. The importance of the normalized equations to only two parameters is that the two parameters can be used to identify all the equivalent FEL experiments. The normalized equations provide a better understanding of the trade off among all the FEL design variables.

III. Low Gain Regime with Space Charge Effects

We will now consider the low gain or interference regime without applying any efficiency enhancement schemes. We may expect that the single pass efficiency will be small which implies that we may set $h(\tilde{z},\tilde{t}_0) = \gamma_z(\tilde{z}, \tilde{t}_0)/\gamma_{z0}$ equal to unity without loss of accuracy. The fact that $h(\tilde{z}, \tilde{t}_0) \approx 1$ further implies that both $|\Delta k(\tilde{z})/k_0(0)|$ and $|\partial\psi(\tilde{z}, \tilde{t}_0)/\partial\tilde{z}|$ are much less than unity. With these assumptions the non-linear FEL equations in (8) become

$$\frac{\partial^2\psi(\tilde{z}, \tilde{t}_0)}{\partial\tilde{z}^2} = \frac{d\delta k(\tilde{z})}{d\tilde{z}} + C_0^2 a(0) \sin\psi(\tilde{z}, \tilde{t}_0)$$

$$+ 2\pi D_0^2(\langle\cos\psi(\tilde{z}, \tilde{t}_0)\rangle\sin\psi(\tilde{z}, \tilde{t}_0) - \langle\sin\psi(\tilde{z}, \tilde{t}_0)\rangle\cos\psi(\tilde{z}, \tilde{t}_0)), \quad (12a)$$

$$\delta k(\tilde{z})a(\tilde{z}) = -2\pi\langle\cos\psi(\tilde{z}, \tilde{t}_0)\rangle , \quad (12b)$$

$$\frac{da(\tilde{z})}{d\tilde{z}} = -2\pi\langle\sin\psi(\tilde{z}, \tilde{t}_0)\rangle . \quad (12c)$$

Since we are considering the low gain regime, a(z) is replaced by a(0) on the right hand side of (8a).

We seek for solutions where space charge effect is moderately important. To solve for the linear dynamics we expand $\psi(\tilde{z}, \tilde{t}_0)$ by setting $\psi(\tilde{z}, \tilde{t}) = \psi^{(0)}(\tilde{z}, \tilde{t}_0) + \psi^{(1)}(\tilde{z}, \tilde{t}_0) + \psi^{(2)}(\tilde{z}, \tilde{t}_0)$, where $\psi^{(0)} > \psi^{(1)} > \psi^{(2)}$. The equations we will solve are

$$\frac{\partial^2\psi^{(0)}(\tilde{z},\tilde{t}_0)}{\partial\tilde{z}^2} = 0 , \quad (13a)$$

$$\frac{\partial^2\psi^{(1)}(\tilde{z}, \tilde{t}_0)}{\partial\tilde{z}^2} = C_0^2 a(0)\sin\psi^{(0)}(\tilde{z}, \tilde{t}_0) , \quad (13b)$$

$$\frac{\partial^2\psi^{(2)}(\tilde{z}, \tilde{t}_0)}{\partial\tilde{z}^2} = \frac{d\delta k(\tilde{z})}{d\tilde{z}} \quad (13c)$$

$$+ 2\pi D_0^2(\langle\cos(\psi^{(0)} + \psi^{(1)})\rangle\sin\psi^{(0)}(\tilde{z}, \tilde{t}_0) - \langle\sin(\psi^{(0)}+\psi^{(1)})\rangle\cos\psi^{(0)}(\tilde{z},\tilde{t}_0).$$

The solutions are

$$\psi^{(0)}(\tilde{z},\tilde{t}_0) = \tilde{t}_0 + \mu\tilde{z} \ , \tag{14a}$$

$$\psi^{(1)}(\tilde{z},\ \tilde{t}_0) = -\ C_0^2\ \frac{a(0)}{\mu^2}(\sin(\tilde{t}_0+\mu\tilde{z}) - \sin\ \tilde{t}_0 - \mu\tilde{z}\ \cos\ \tilde{t}_0) \ , \tag{14b}$$

$$\psi^{(2)}(\tilde{z},\ \tilde{t}_0) = \frac{C_0^2\ \pi}{\mu^3}(2\ \sin\ \mu\tilde{z} - \mu\tilde{z}\ \cos\ \mu\tilde{z} - \mu\tilde{z}) \tag{14c}$$

$$-\ \pi\ \frac{C_0^2\ D_0^2\ a(0)}{\mu^4}\left\{\sin(\tilde{t}_0+\ \mu\tilde{z}) - \sin\ \tilde{t}_0 - \mu\tilde{z}\cos\tilde{t}_0 + \frac{\mu^2\tilde{z}^2}{2}\ \sin\ \tilde{t}_0 + \frac{\mu^3\tilde{z}^3}{6}\ \cos\ \tilde{t}_0\right\}$$

where $\mu = -\ \Delta\omega/\omega_0$

Substituting (14) into (12c) and integrating over $\tilde{z}$ we find that the gain G with space charge effects is given by

$$G(\theta,\theta_p) = \frac{-\pi^{\frac{1}{2}}C_0^2\tilde{z}^2}{4D_0}\ S(\theta,\theta_p) \ , \tag{15}$$

where

$$S(\theta,\theta_p) = 2\left[\theta_p\ \frac{\partial}{\partial\theta} + \frac{1}{3!}\ \theta_p^3\ \frac{\partial^3}{\partial\theta^3}\right]\left[\frac{\sin\theta}{\theta}\right]^2$$

$\theta = \mu\tilde{z}/2$ and $\theta_p = \pi^{\frac{1}{2}}\ D_0\tilde{z}/2 = \sqrt{F_{sc}/F_{em}}\ \ \xi\tilde{z}/2\gamma_{z0}$ is the contribution due to space charge effects. For $\theta_p < \theta$, we can rewrite (15) as

$$S(\theta,\theta_p) = \left[\frac{\sin(\theta+\theta_p)}{\theta+\theta_p}\right]^2 - \left[\frac{\sin(\theta-\theta_p)}{\theta-\theta_p}\right]^2 . \tag{16}$$

When space charge effects are negligible, the maximum gain occurs at $\theta = 1.3$ where $\partial(\sin\theta/\theta)^2/\partial\theta = 0.54$ and is

$$G_{max}(z) = \left[\frac{\beta_{0\perp}\xi}{4}\right]^2 (k_0(0)z)^3 << 1 \tag{17}$$

We can estimate the level of electromagnetic field needed to achieve saturation in an interaction length L. Electron trapping and thus saturation occurs when the phase shift of the particles with respect to the wave is approximately π. Loosely speaking, saturation occurs when $|\psi^{(1)}(\tilde{z},\tilde{t}_0)| \approx \pi$, using (12b) we find that this condition gives $a(0) \approx 2\pi/(C_0^2k_0^2L^2)$ or

$$A(0) \approx \frac{\pi}{2} \frac{A_0}{(\beta_{0\perp} \gamma_{z0} k_0 L)^2} \tag{18}$$

This value of the radiation field, necessary to achieve saturation at z = L is to within a numerical factor of order unity, the same as that obtained in Ref. (24) using a different line of reasoning.

The gain expression with space charge effect is valid when $1 \gg \theta_p^2$, in order that the assumption $\psi^{(1)} \gg \psi^{(2)}$ is satisfied. Therefore, the gain expression is applicable when the space charge effect is only moderately important. The condition for space charge to be important is

$$\theta_p^2 = \frac{F_{sc}}{F_{em}} \left(\frac{\xi k_0(0) z}{2\gamma_{z0}} \right)^2 \gg 1 \tag{19}$$

where $\xi = \sqrt{F_{em}}\ \omega_0 / (\sqrt{\gamma_0}\ ck_0(0))$. For $F_{sc} = F_{em} = 1$, this condition is identical to that derived in Refs. (37) and (38). Condition (19) is dependent on the length of the interaction region L. Space charge effect becomes important when $L \geq (2\gamma_{z0}/\xi k_0(0))\ (F_{em}/F_{sc})^{\frac{1}{2}}$.

The more appropriate condition for neglecting space charge effect is

$$\frac{2\pi D_0^2}{C_0^2 a(0)} \lesssim 1 \tag{20}$$

The physical interpretation of Eq. (20) is that space charge effects become important when the ideal maximum amplitude of the space charge potential becomes much larger than the initial amplitude of the ponderomotive potential. This condition, rewritten in terms of the electron density is

$$n_0 \lesssim (k_0^2 \gamma_{z0}^2 A_0 A)\ (2\pi \gamma_0 m_0 c^2 F_{sc})^{-1}. \tag{21}$$

The condition for neglecting space charge effects Eq. (20) is not directly related to the length of the interaction region, but dependent on the amplitude of the vector potential of the radiation. For the low gain case, using Eq. (18) as the approximate initial amplitude of the radiation vector potential for obtaining saturation at length L, Eq. (20) reduces to Eq. (19) to within a numerical factor of order unity.

The linear gain expression should always be used with discretion. The linear gain expression is valid before saturation effects becomes important. When the frequency mismatch is small,

$$0 < \frac{-\Delta\omega}{\omega_0} < \frac{\Delta\gamma}{\gamma_0}\Big|_{trap} \tag{22}$$

some particles can be initially trapped in the ponderomotive well. The full width of the trapping potential is given by

$$\frac{\Delta\gamma}{\gamma_0}\Big|_{trap} = \frac{|e|\phi_{trap}}{\gamma_0 m_0 c^2} = 2\sqrt{C_0^2 a(0)} \tag{23}$$

When particles are initially trapped, saturation effects become important roughly within a distance of half of a bounce wavelength. A bounce wavelength, L_b, is the distance the trapped electrons travel in the axial direction while executing a bounce period in the ponderomotive potential well. Considering only nearly resonant particles in Eq. (8a), we find

$$\frac{1}{2}\frac{L_b}{\ell_0} = \left(C_0^2 a(0)\right)^{-\frac{1}{2}} . \tag{23}$$

If the frequency mismatch satisfy the inequality Eq. (22), the linear gain expression is valid for $\tilde{z}/2\pi << \frac{1}{2} L_b/\ell_0$.

For the low gain regime, the independent non-dimensional parameters are $C_0^2 a(0)$, $\Delta\omega/\omega_0$ and D_0^2. The appropriate dependent variables are a(0)G and η. In the low gain regime, the efficiency is approximately

$$\eta \simeq \frac{1}{4\pi}\left(1+\frac{\Delta\omega}{\omega_0}\right)\left(C_0^2\, a(0)\right)\left(a(0)\, G\quad\right). \tag{24}$$

IV. Numerical Results

We will apply our theory to illustrate a few concepts on space charge effects and filling factors using a practical example in the low gain regime. We will also present some widely applicable graphs for growth rate and efficiency in the high gain regime.

a) Low Gain Example

The FEL experiment we have chosen consists of a magnetic wiggler with a wavelength ℓ_0= 1 cm (k_0= 2π cm^{-1}), amplitude B_0= 325 gauss (A_0 = 51.7 stat volts), an interaction length L = 3 m, an electron beam with energy of 3 Mev (γ_0= 7) and current density of 16A/cm^2 (n_0= 3.3 x $10^9 em^{-3}$, ω_b= 3.3 x $10^{-9} sec^{-1}$). The radiation is at 102 μm[36]. Taking filling factors to be unity, we obtain ξ = 6.5 x 10^{-3} and $\beta_{0\perp}$ = 4.33 x 10^{-3}. For the initial example, A(0) is chosen to achieve saturation at z=L as predicted by linear theory[24]. For the parameters here, A(0) = A_L = 3.5 x 10^{-2}stat volts. The normalized parameters are $C_0^2 a(0)$ = 2.5 x 10^{-6} and D_0^2 = 2.85 x 10^{-7}.

Figure 2 consists of plots of linear gain with space charge effects (solid curve), θ_p^2 = 0.76, and linear gain without space charge effects, (dashed curve), θ_p^2 = 0, as a function of the frequency mismatch $\Delta\omega/\omega_0$ at $\tilde{z}/2\pi$ = 300 (z = 3m). We see that space charge effects reduce the linear gain by about 20% at the maximum. The dotted curve is the gain

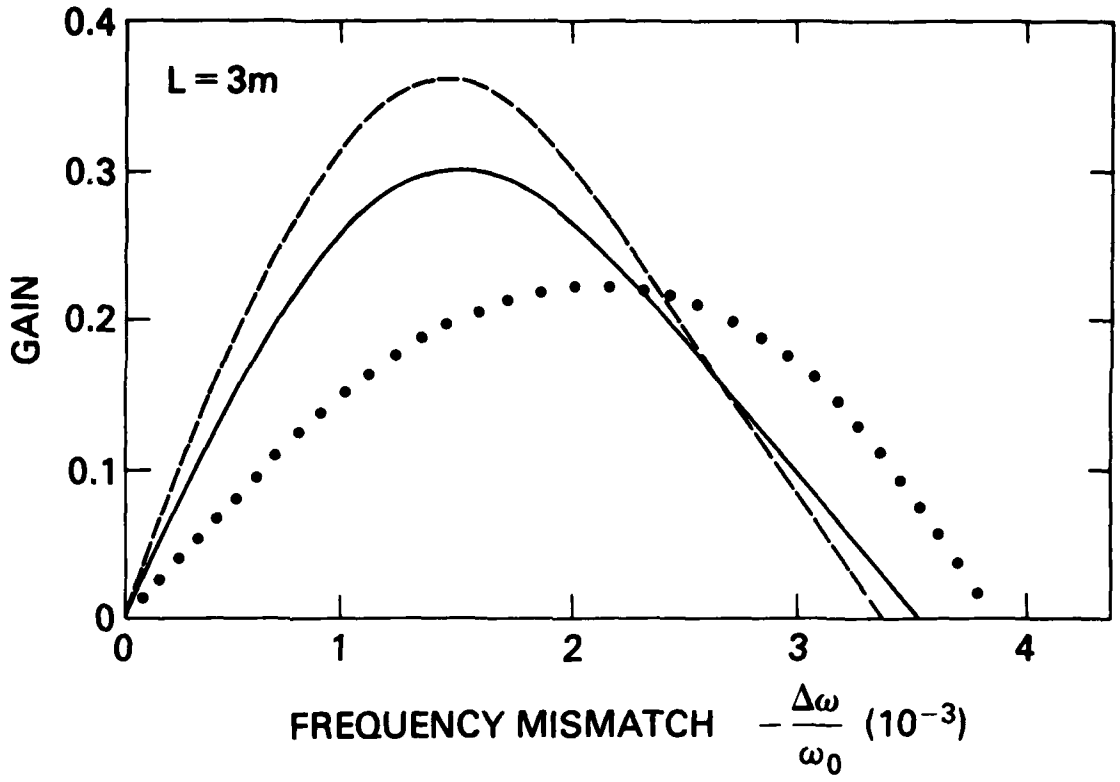

Fig. 2 — Plots of gain as a function of frequency mismatch, $\Delta\omega/\omega_o$ at 3m. The solid curve is linear gain with space charge effects, $\theta_p{}^2 = 0.76$. The dashed curve is linear gain without space charge effects, $\theta_p{}^2 = 0$, and the dotted curve is the gain at 3m calculated from the non-linear self-consistent equations (8a-d).

at 3m calculated from the non-linear equations (8a-d), and the peak value of the gain has shifted to a larger frequency mismatch.

If the frequency match is small relative to the trapping potential, as in Eq. (20), saturation effects become important when the electrons travel roughly half of a bounce length. A bounce wavelength L_b is the distance electrons travel in the axial direction while executing a bounce period in the ponderomotive well. For this example, $\frac{\Delta\gamma}{\gamma_0}\Big|_{trap} \simeq 6 \times 10^{-3}$ and $L_b/2 = 3.1$m. Therefore, linear theory is not applicable at 3m. Plots of linear gain with space charge effects (solid curve), linear gain without space charge effects (dashed curve), and gain from non-linear self-consistent calculation (dotted curve) as a function of axial distance

for $\Delta\omega/\omega_0 = -1.5 \times 10^{-3}$ are shown in Fig. 3 . This value of frequency mismatch gives the maximum linear gain at $\tilde{z}/2\pi = 300$ (z=3m) see Fig. 2 . The linear regime of the non-linear self-consistent formulation is $z \leq 2m$ for this example. Finally, we will show that, in the linear regime of the non-linear calculation, the gain from the non-linear calculation is in good agreement with the linear gain expression as shown in Fig. 4 calculated at $\tilde{z}/2\pi = 150$ (z = 1.5m).

To summarize, the disagreement between linear gain and gain from non-linear calculation at z = 3m is that the initial guess of $C_0^2 a(0) = 2.5 \times 10^{-6}$ ($A(0) = A_L$) was slightly too large. Saturation effects have become important at the end of the interaction region. As $C_0^2 a(0)$ or A(0) decreases, the gain from non-linear calculation will converge to the linear gain expression as shown in Fig. 5 . Figure 5 contains curves of the gain from the non-linear formulation (solid curves) for various values of $C_0^2 a(0)$, linear gain with space charge effects (dashed curve), and the gain from non-linear calculation without the space charge potential and $C_0^2 a(0) = 1.25 \times 10^{-6}$ ($A(0) = \frac{1}{2} A_L$)(circles) as a function of frequency mismatch at $\tilde{z}/2\pi = 300$ (z = 3m). In the linear regime of the non-linear calculation, the space charge potential decreases the gain, agreeing with the linear theory. Figure 6 are plots of efficiency versus frequency mismatch at $\tilde{z}/2\pi = 300$ (z = 3m) for the same range of $C_0^2 a(0)$.

The effect of space charge on gain for the same FEL example will be summarized below. According to linear theory , the space charge effect is only moderately important for $\theta_p^2 = 0.76$. We found that the effects of space charge are dependent on the radiation vector potential at input, A(0). Taking $A(0) = A_L$, we obtain $C_0^2 a(0) = 2.5 \times 10^{-6}$ and $\frac{2\pi D_0^2}{C_0^2 a(0)} = 0.67$. The results of self-consistent non-linear calculations found the space

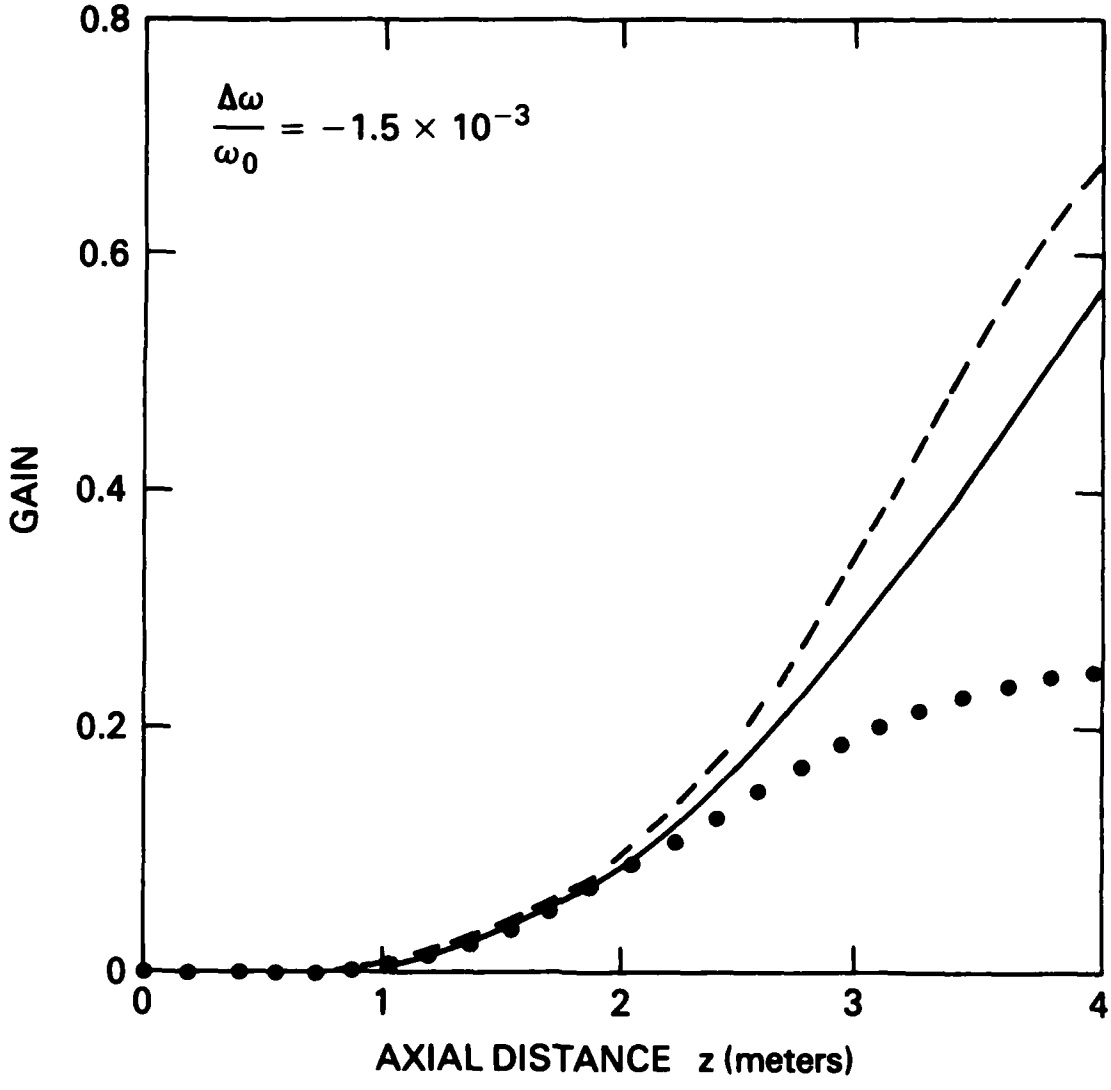

Fig. 3 — Plots of gain as a function of axial position at the frequency mismatch, $\Delta\omega/\omega_o = -1.5 \times 10^{-3}$, which gives the largest value of linear gain. The solid curve is linear gain with space charge effects, $\theta_p^2 = 0.76$. The dashed curve is linear gain without space charge effects, $\theta_p^2 = 0$, and the dotted curve is the gain from the non-linear self-consistent equations (8a-d). Saturation effects are important at 3m.

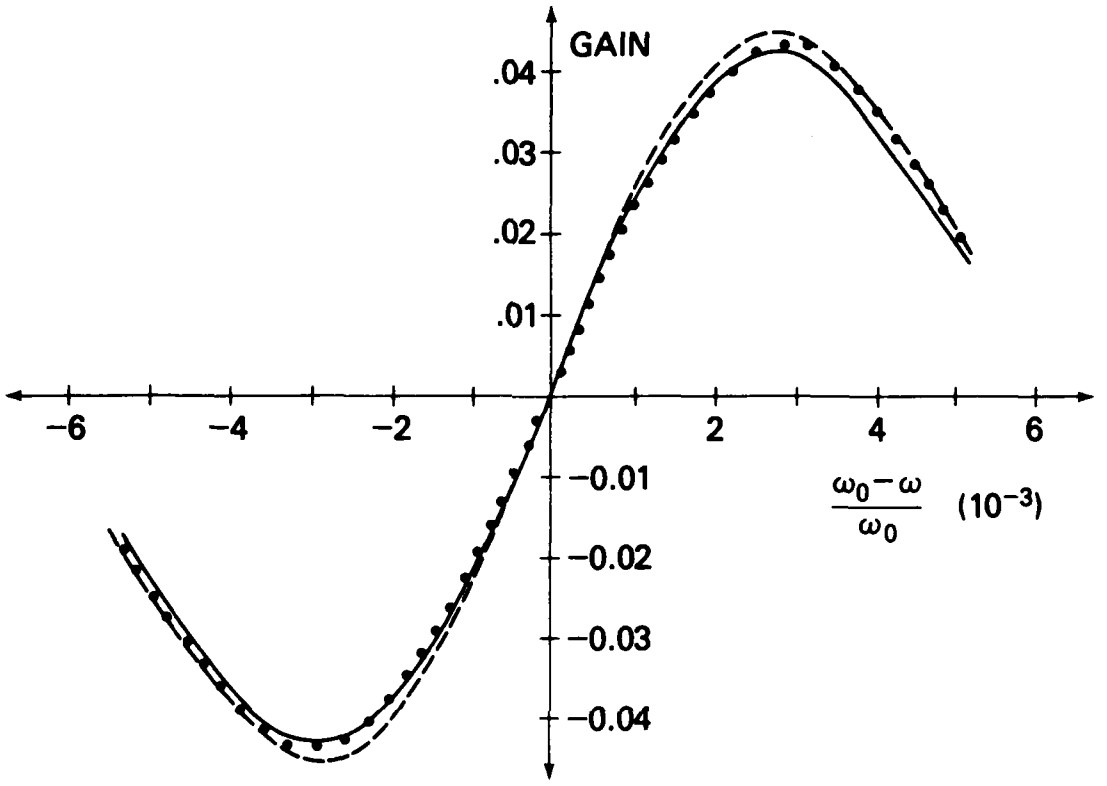

Fig. 4 — Plots of gain as a function of frequency mismatch, $\Delta\omega/\omega_o$, at z = 1.5m, which is within the linear regime of the self-consistent calculation. The solid curve is linear gain with space charge effects, $\theta_p{}^2$ = 0.76. The dashed curve is linear gain without space charge effects, $\theta_p{}^2$ = 0. The dotted curve is the gain from non-linear self-consistent calculations (8a-d).

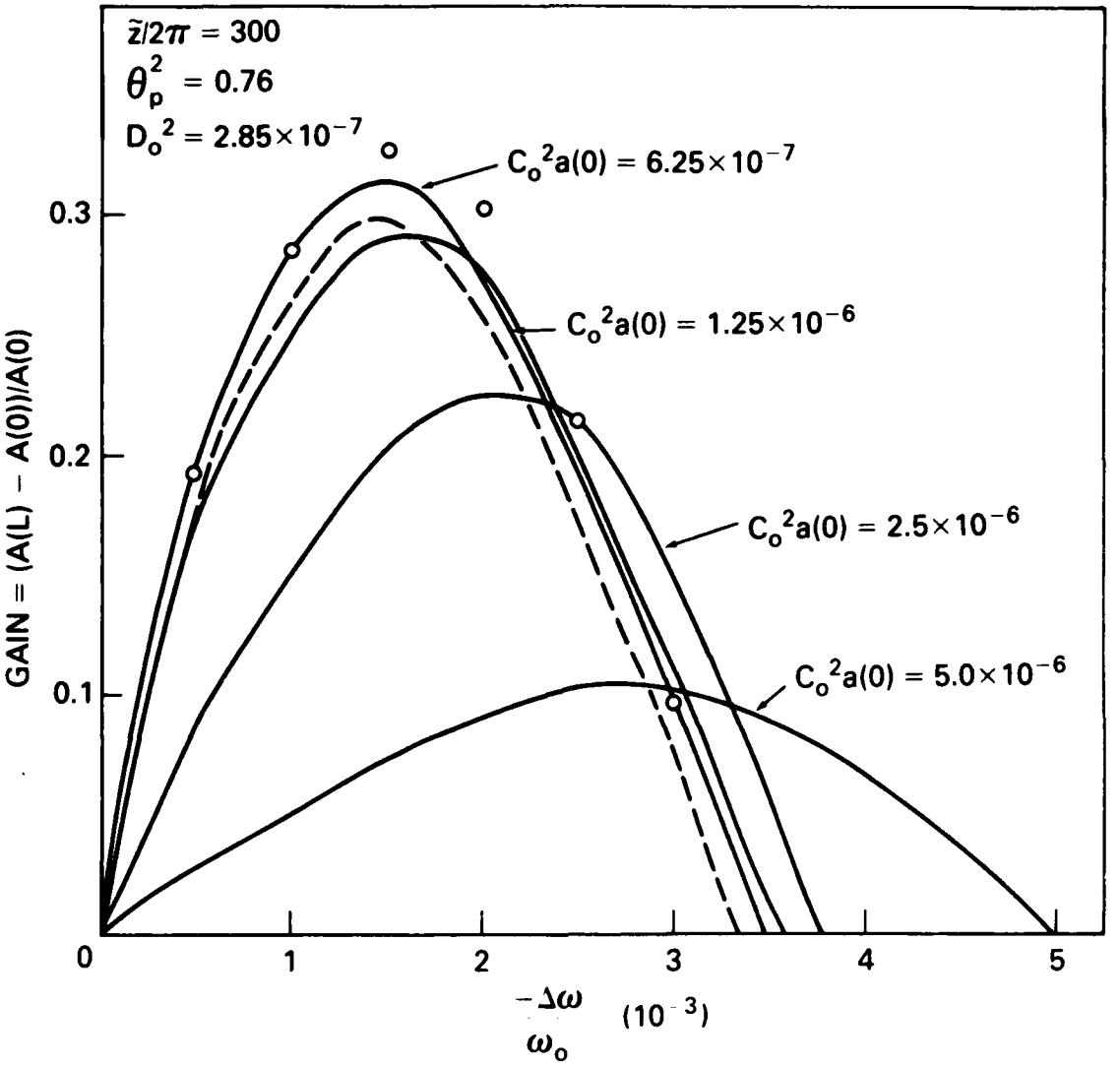

Fig. 5 — Plots of gain as a function of frequency mismatch at $z/2\pi = 300$ (z=3m). The solid curve is gain from non-linear self-consistent formulation for various values of $C_o^2a(0)$. The dashed curve is linear gain with space charge effects, and circles (o) are gain from non-linear self-consistent calculation without space charge effects with $C_o^2a(0) = 1.25 \times 10^{-6}$.

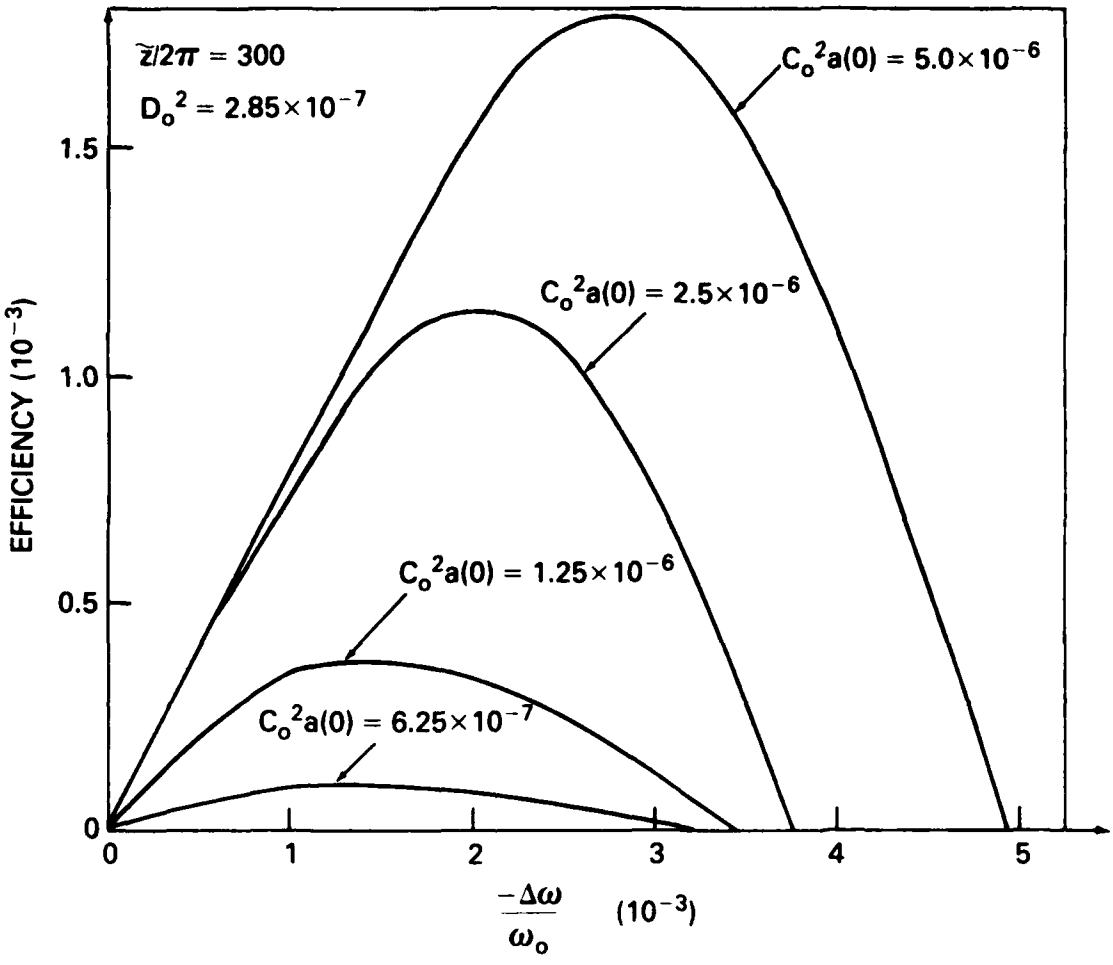

Fig. 6 — Plots of efficiency versus frequency mismatch at $\tilde{z}/2\pi = 300$ (z=3m) for various values of $C_o^2a(0)$

charge effects to be negligible. Space charge effects become increasingly more important as we decrease $C_0^2 a(0)$ or $A(0)$. In Fig. 5 , we see that the gain in the linear regime of the non-linear calculation without the space charge effects (circles (o) is about 10% larger for $C_0^2 a(0) = 1.25 \times 10^{-6}$ ($A(0) = 1/2\ A_L$) and $\frac{2\pi D_0^2}{C_0^2 a(0)} = 1.3$. Figure 7 contains curves of the spatial evolution of the amplitude of the space charge potential (dashed curve) and the amplitude of the ponderomotive potential (solid curve) for $\Delta\omega/\omega_0 = -2.0 \times 10^{-3}$, $C_0^2 a(0) = 1.25 \times 10^{-6}$ ($A(0) = 1/2\ A_L$) and $D_0^2 = 2.85 \times 10^{-7}$. Notice that at 3m, the space charge potential is about 2/3 of the ponderomotive potential. Thus we expect the space charge potential to have a moderate effect on the gain.

Figure 8 contains plots of gain with space charge effects (solid curve) and gain without space charge effects (dashed curve) as a function of axial distance for $\frac{\Delta\omega}{\omega_0} = -2.0 \times 10^{-3}$, $C_0^2 a(0) = 1.25 \times 10^{-6}$ ($A(0) = 1/2\ A_L$) and $D_0^2 = 2.85 \times 10^{-7}$. As noted in Fig. 5, the space charge effects decrease the gain in the linear regime of the self-consistent calculation. The collective effects of the space charge field, however, increase the gain in the non-linear regime.

Let us now turn our attention toward the effects of filling factors. When the electromagnetic filling factor F_{em} is no longer equal to unity, the appropriate parameter for comparison purposes is efficiency as expressed by Eq. (11a). Plots of efficiency versus axial distance for various combination of filling factors are shown in Fig. 9 for $\frac{\Delta\omega}{\omega_0} = -2.0 \times 10^{-3}$, $C_0^2 a(0) = 1.25 \times 10^{-6}$ and $D_0^2/F_{sc} = 2.85 \times 10^{-7}$. In the linear regime, $\tilde{z}/2\pi < 300$ the efficiencies calculated with different filling factors are approximately the same. In the non-linear regime $\tilde{z}/2\pi > 300$, efficiency became smaller as F_{em} decreases.

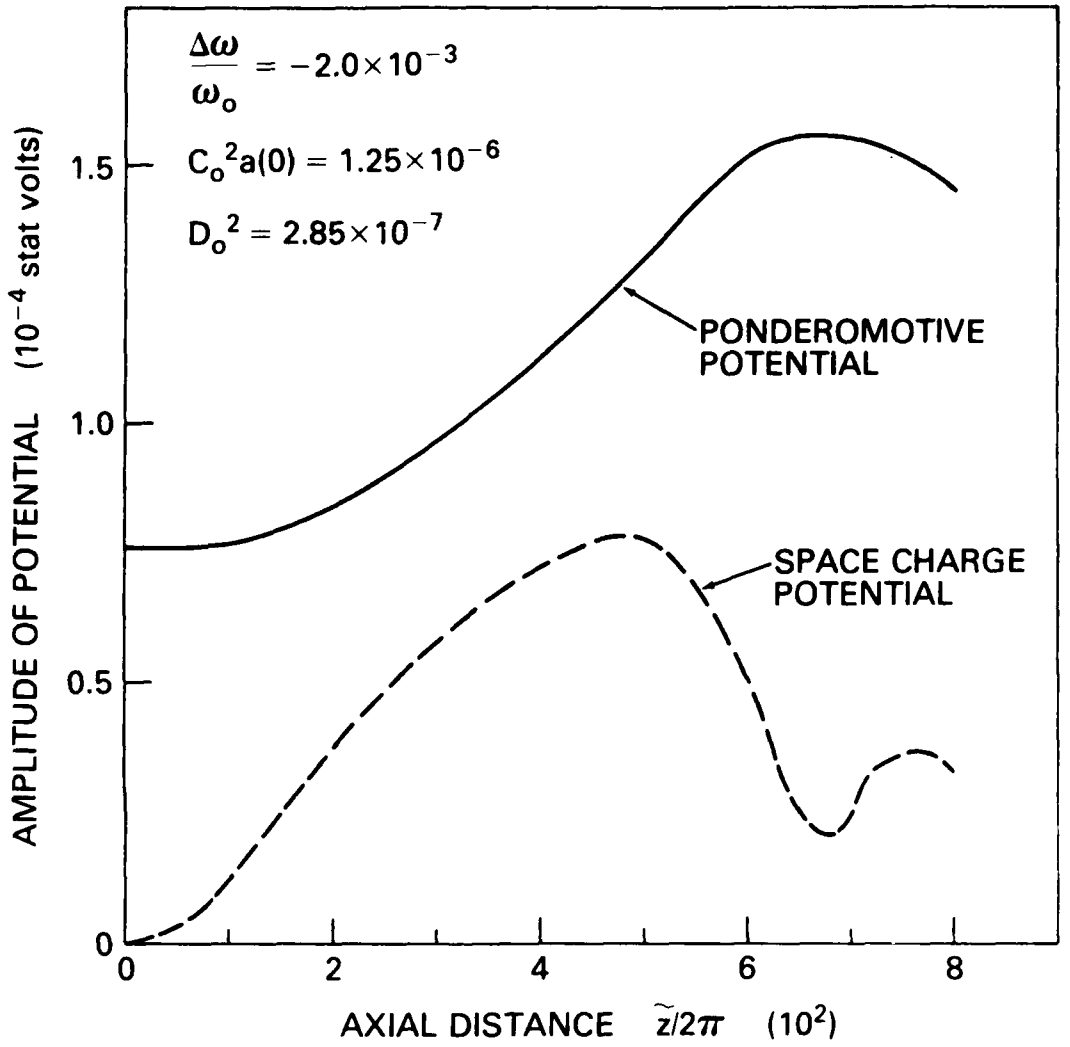

Fig. 7 — Plots of the amplitude of the space charge potential (dashed curve) and the amplitude of the ponderomotive potential (solid curve) as a function of axial position for $\Delta\omega/\omega_o = -2.0 \times 10^{-3}$, $C_o^2 a(0) = 1.25 \times 10^{-6}$ ($A(0) = 1/2\ A_L$) and $D_o^2 = 2.85 \times 10^{-7}$

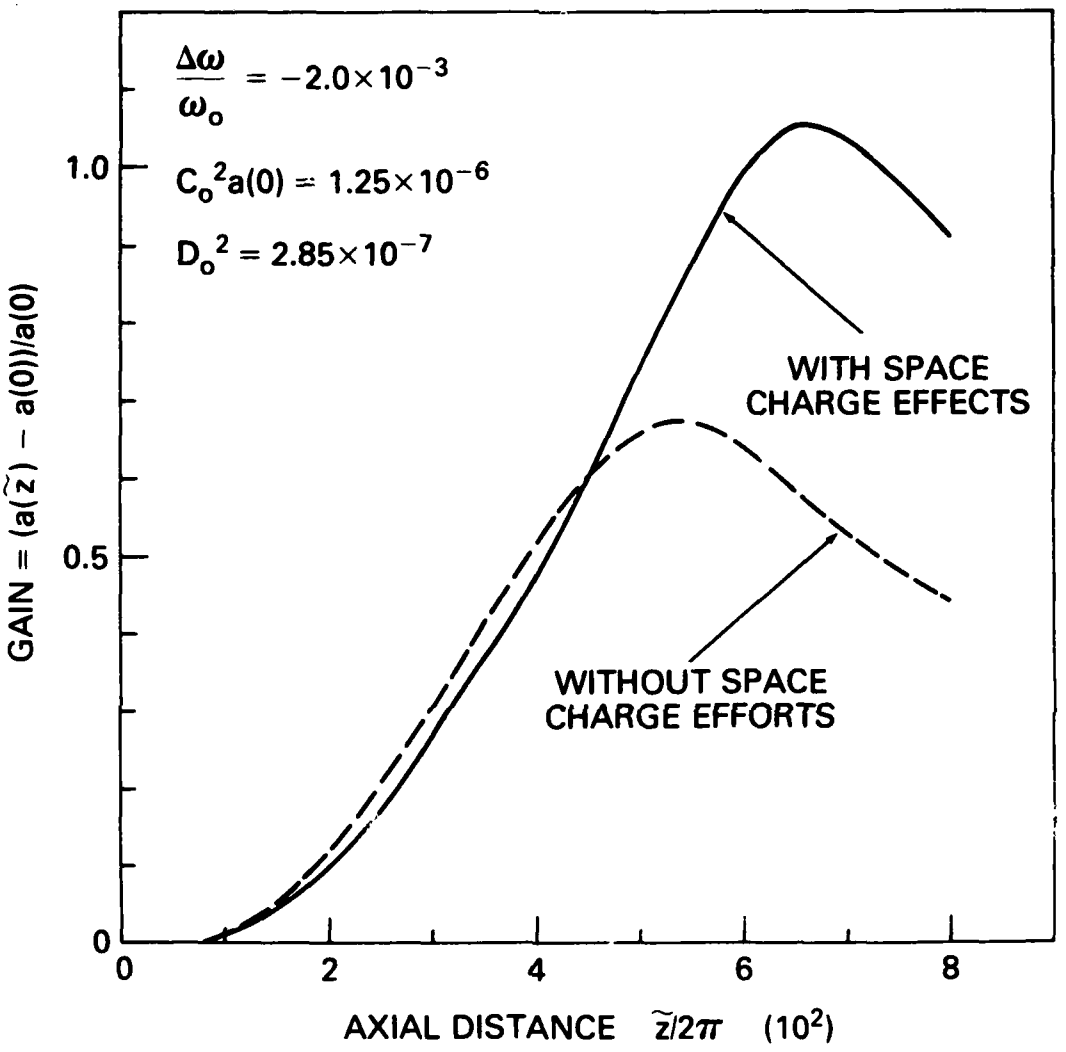

Fig. 8 — Plots of gain with space charge effects (solid curve) and gain without space charge effects (dashed curve) as a function of axial distance for $\Delta\omega/\omega_o = -2.0 \times 10^{-3}$, $C_o^2 a(0) = 1.25 \times 10^{-6}$ ($A(0) = 1/2\ A_L$) and $D_o^2 = 2.85 \times 10^{-7}$

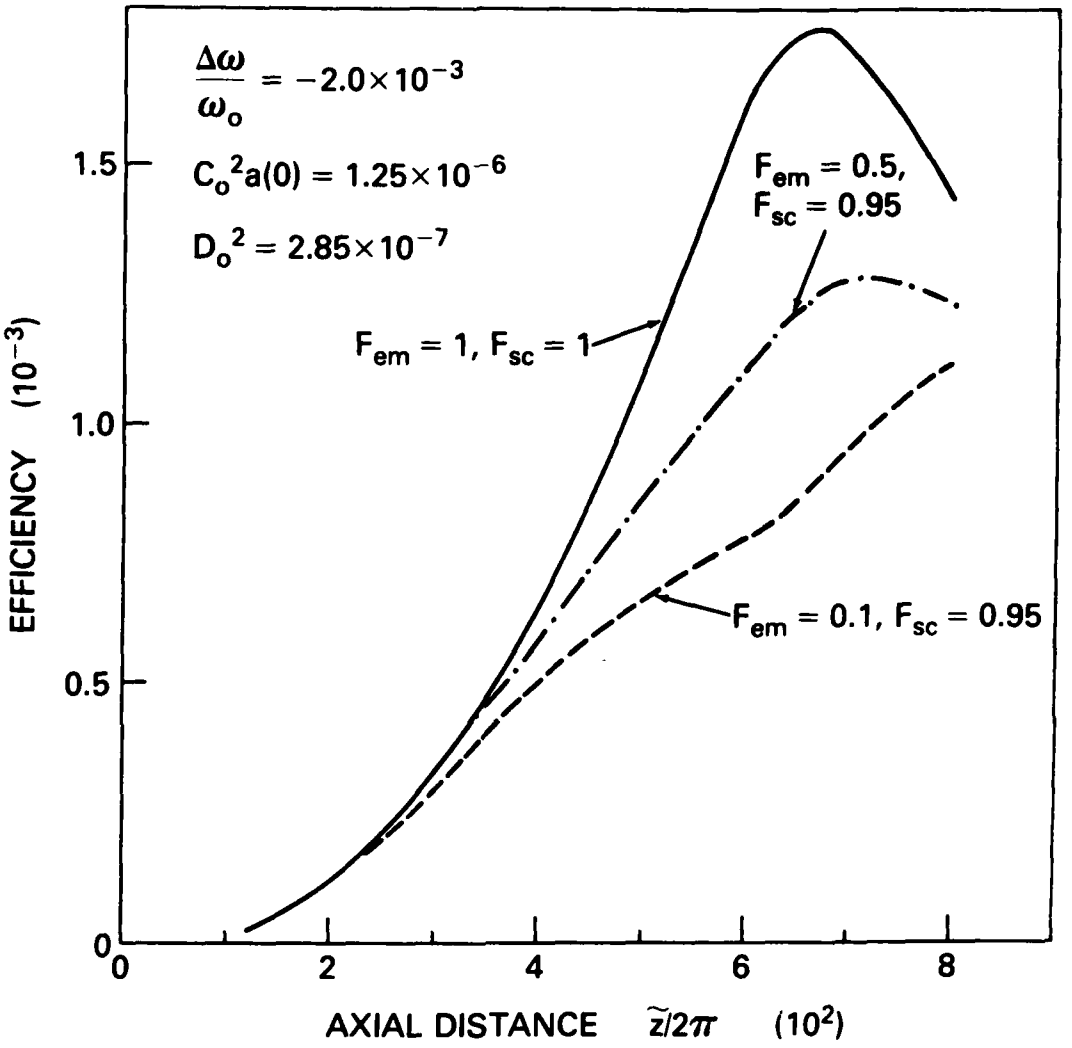

Fig. 9 — Plots of efficiency versus axial distance for various combination of filling factors with $\Delta\omega/\omega_o = -2.0 \times 10^{-3}$, $C_o^2 a(0) = 1.25 \times 10^{-6}$, and $D_o^2/F_{sc} = 2.85 \times 10^{-7}$

In the low gain regime the non-dimensional value a(0)G at any axial position $\tilde{z}$ is only a function of the independent parameters $C_0^2 a(0)$, D_0^2 and $\Delta\omega/\omega_0$. A set of three curves of a(0)G at saturation for different non-dimensional values of $C_0^2 a(0)$ is shown as a function of frequency mismatch, $\Delta\omega/\omega_0$, in Fig. 10 for $D_0^2 = 2.85 \times 10^{-7}$.

b) <u>High Gain Regime</u>

For the high gain regime, we illustrate examples where collective effects are negligible. Figure 11 is a plot of growth rate in the linear regime of the non-linear self-consistent formulation as a function of frequency mismatch with $D_0^2 = 5 \times 10^{-7}$ and various values of C_0^2. The results are in good agreement with the normalized linear growth rate obtained from linear dispersion relation, Eq. (10). The saturation amplitude and efficiency as a function of frequency mismatch are plotted in Figures 12 and 13. We notice that the magnitude of efficiency as well as the bandwidth increases as C_0^2 increases.

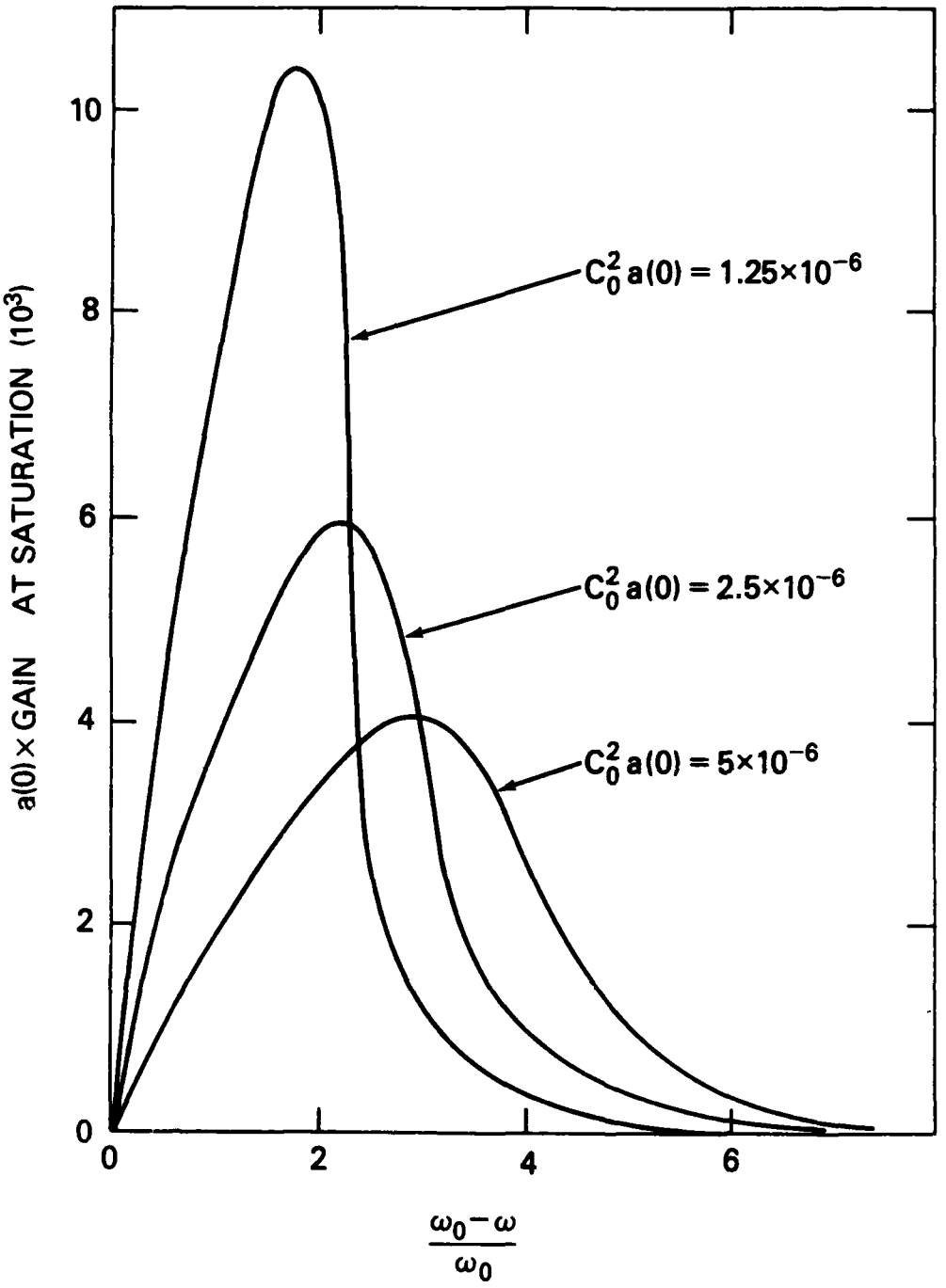

Fig. 10 — Plots of $\tilde{a}(0)G$ at the saturation in the low gain regime of the non-linear self-consistent calculations, when space charge effect is moderately important, $D_o^2 = 2.85 \times 10^{-7}$, as a function of the non-dimensional parameters $C_o^2 a(0)$ and $\Delta\omega/\omega$

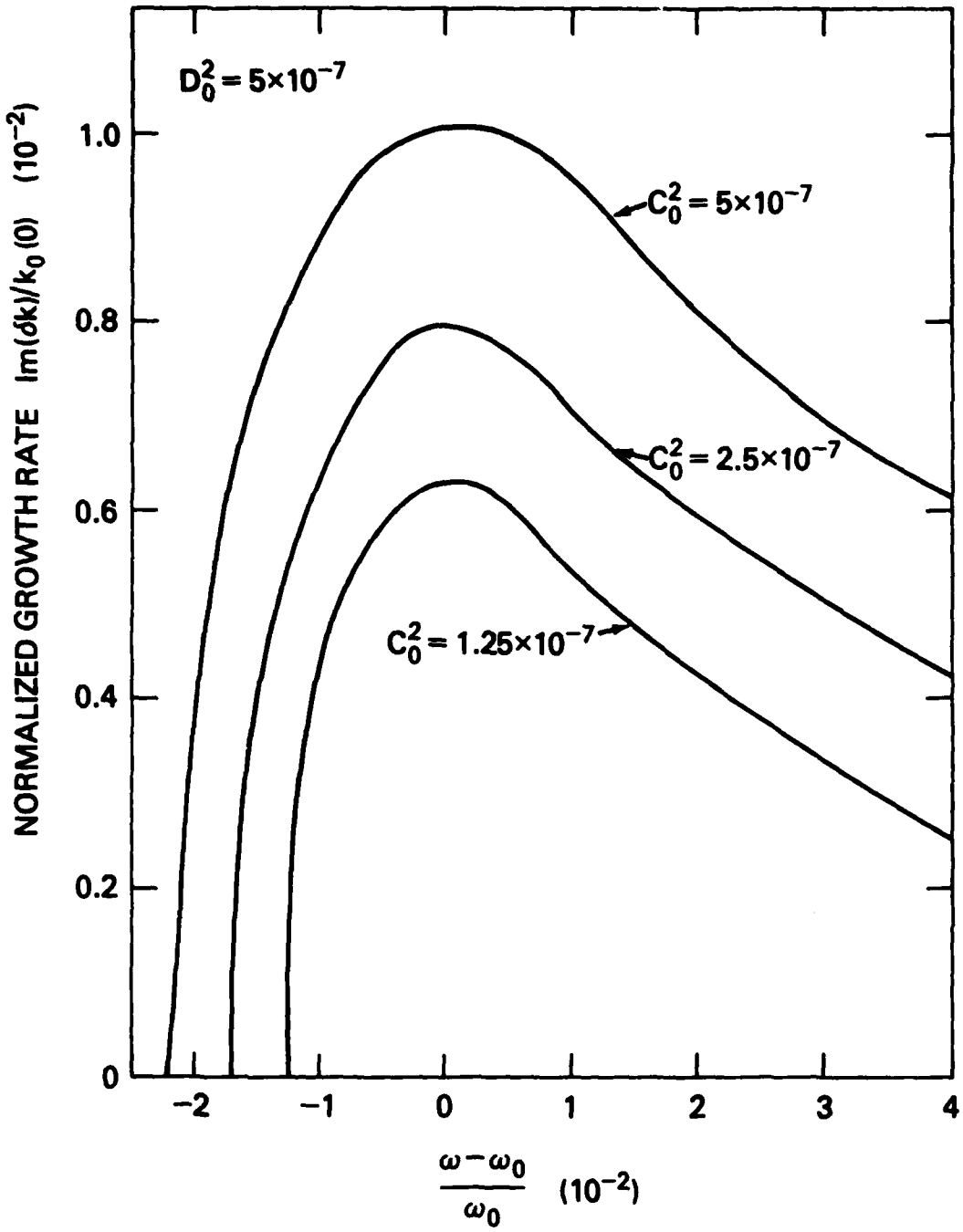

Fig. 11 — Plots of linear growth rate in the high gain regime, where collective effects are negligible, $D_o^2 = 5 \times 10^{-7}$ as a function of frequency mismatch $\Delta\omega/\omega$ and C_o^2

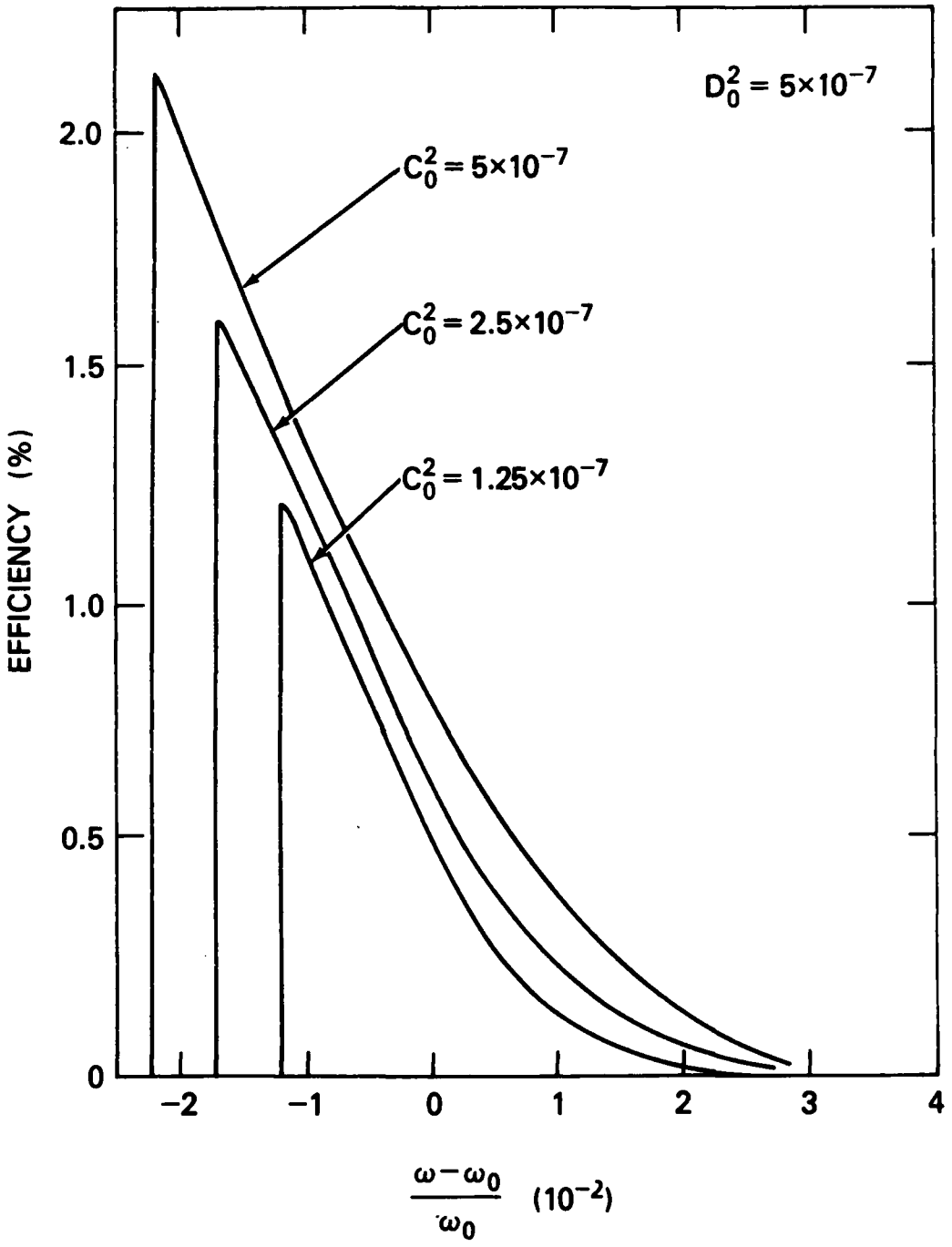

Fig. 12 — Plots of efficiency in the high gain regime as a function of frequency mismatch $\Delta\omega/\omega_o$ and C_o^2 for a case when the collective effect is negligible, $D_o^2 = 5 \times 10^{-7}$

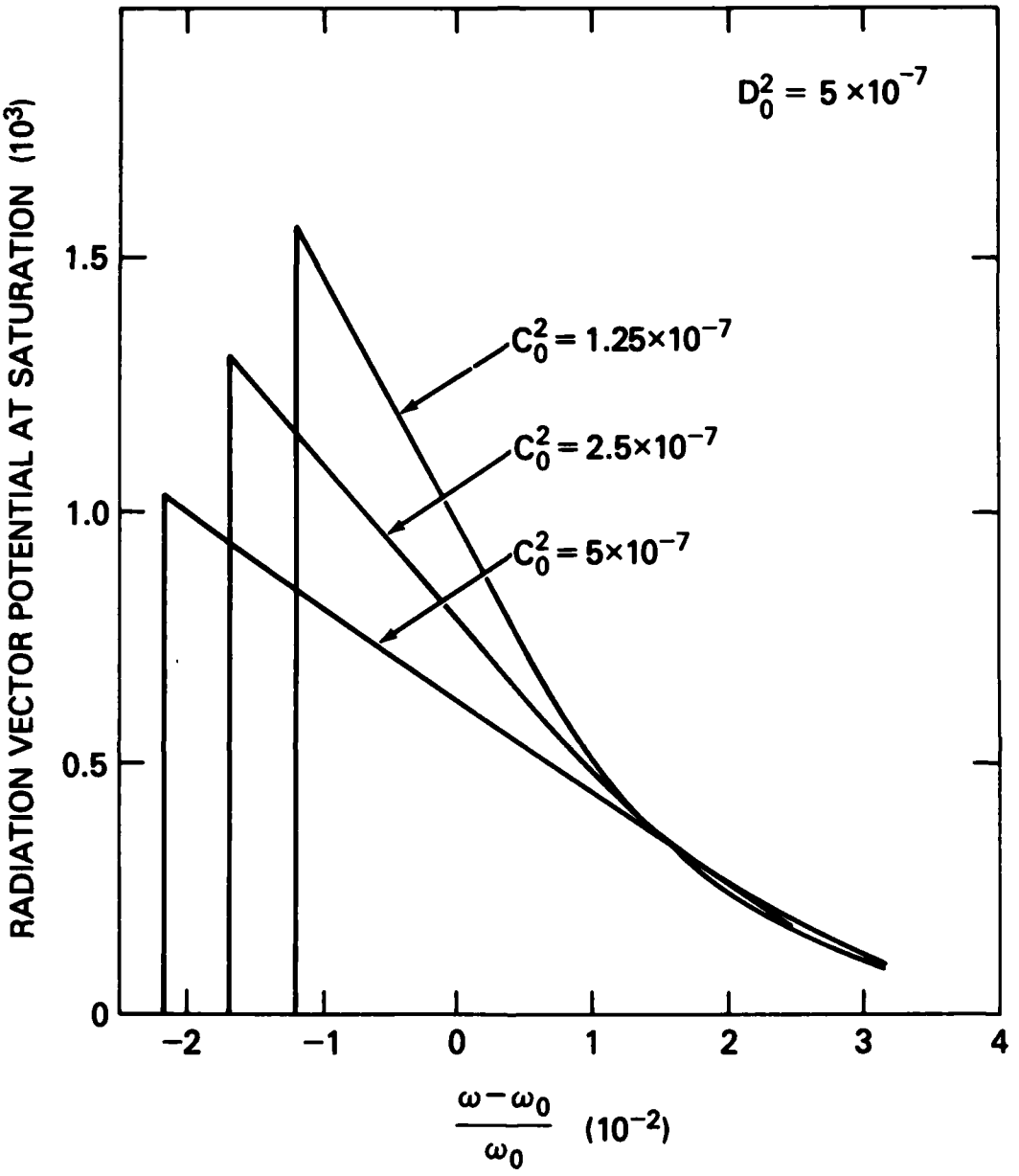

Fig. 13 — Plots of saturation amplitude of the radiation vector potential in the high gain regime as a function of frequency mismatch $\Delta\omega/\omega_o$ and C_o^2 when the collective effect is negligible, $D_o^2 = 5 \times 10^{-7}$

ACKNOWLEDGMENTS

The authors appreciate useful discussions with I. B. Bernstein and W. M. Manheimer. The authors would also like to acknowledge the support for this work by DARPA under Contract No. 3817.

REFERENCES

1. H. Motz, J. Appl. Physics. 22, 527 (1951).
2. J. M. J. Madey, J. Appl. Phys. 42, 1906 (1971).
3. R. B. Palmer, J. Appl. Phys. 43, 3014 (1972).
4. V. P. Sukhatme and P. W. Wolff, J. Appl. Phys. 44, 2331 (1973).
5. J. M. J. Madey, H. A. Schwettman and W. M. Fairbank, IEEE Trans. Nucl. Sci. 20, 980 (1973).
6. A. T. Lin and J. M. Dawson, Phys. Fluids 18, 201 (1975).
7. A. Hasegawa, K. Mima, P. Sprangle, H. H. Szu and V. L. Granatstein, Appl. Phys. Lett. 29, 542 (1976).
8. F. A. Hopf, P. Meystre, M. O. Scully and W. H. Louisell, Phys. Rev. Lett. 37, 1342 (1976).
9. F. A. Hopf, P. Meystre, M. O. Scully and W. H. Louisell, Optics Comm. 18, 413 (1976).
10. W. B. Colson, Phys. Lett. 59A, 187 (1976).
11. N. M. Kroll and W. A. McMullin, Phys. Rev. A17, 300 (1978).
12. P. Sprangle and V. L. Granatstein, Phys. Rev. A17, 1792 (1978).
13. S. B. Segall, Report No. KMSF-U806 Oct. (1978).
14. L. R. Elias, Phys. Rev. Lett. 42, 977 (1979).
15. P. Sprangle and A. T. Drobot, J. Appl, Phys. 50, 2652 (1979).
16. P. Sprangle and V. L. Granatstein, Appl. Phys. Lett. 25, 377 (1974).

17. W. M. Manheimer and E. Ott, Phys. Fluids 17, 706 (1974).

18. V. I. Miroshnickenko, Sov. Tech. Phys. Lett. 1, 453, (1975).

19. P. Sprangle, V. L. Granatstein and L. Baker, Phys. Rev. A12, 1697 (1975).

20. T. Kwan, J. M. Dawson and A. T. Lin, Phys. Fluids 20, 581 (1977).

21. V. L. Granatstein and P. Sprangle, IEEE Trans. MIT-25, 545 (1977).

22. A. Hasegawa, Bell System Tech. J. 57, 3069 (1978).

23. I. B. Bernstein and J. L. Hirshfield, Phys. Rev. Lett. 40, 761 (1978).

24. P. Sprangle, R. A. Smith and V. L. Granatstein, NRL Memo Report 3911 (1978). (Also published in Infrared and Millimeter Waves, Vol. 1, K. Button (ed.), Academic Press, 1979).

25. P. Sprangle and R. A. Smith, NRL Memo Report 4033 (1979), and Phys. Rev. A21, 293 (1980).

26. P. Sprangle, Cha-Mei Tang and W. M. Manheimer, Phys. Rev. Lett. 43, 1932 (1979) and Phys. Rev. A21, 302 (1980).

27. P. Sprangle and Cha-Mei Tang, Proc. of the Fourth Intl. Conf. on Infrared and Near-Millimeter Waves, page 98, Miami Beach, 10-15 December 1979.

28. N. M. Kroll, P. Morton and M. N. Rosenbluth, JASON Tech. Report JSR-79-15 (1980).

29. A. T. Lin and J. M. Dawson, Phys. of Fluids, 23, 1224 (1980).

30. L. Friedland and J. L. Hirshfield, Phys. Rev. Lett. 44, 1456 (1980).

31. Free-Electron Generators of Coherent Radiation, Physics of Quantum Electronics, Vol. 7, edited by S. F. Jacobs, H. S. Pilloff, M. Sargent, III, M. O. Scully and R. Spitzer, Addison-Wesley, Reading, MA. (1980).

32. Efficiency enhancement using a D.C. accelerating electric field has been discussed by i) P. Sprangle and Cha-Mei Tang, DARPA FEL Review, Arlington, VA., Dec. 3-4, 1979, ii) P. Sprangle and Cha-Mei Tang, DARPA/ONR/AFOSR FEL Program Review, LASL, April 24-25, 1980, and iii)

Y. P. Ho, Y. C. Lee and M. N. Rosenbluth, Sherwood meeting, Tucson, Arizona, April 23-25, 1980.

33. P. Sprangle and Cha-Mei Tang, AIAA 13th Fluid and Plasma Dynamics Conf. paper #AIAA-80-1404, Snowmass, Colorado, July 14-16, 1980.

34. P. Sprangle and Cha-Mei Tang, NRL Memo 4280 (1980).

35. A. T. Lin, Report No. PPG-456, Center of Plasma Physics and Fusion Energy, UCLA, January (1980).

36. Luis R. Elias, "The UCSB FEL Experimental Program", QIFEL005/80, Quantum Institute, University of California at Santa Barbara, presented at Int'l School of Quantum Electronics, Erice, Sicily, Italy, 17-29 August (1980).

37. A. Gover and Z. Livni, Opt. Comm., 26, 375 (1979).

38. W. H. Louisell, J. F. Lam, and D. A. Copeland, Phys. Rev. A18, 655 (1978).

DISTRIBUTION LIST*

Naval Research Laboratory
4555 Overlook Avenue, S.W.
Washington, D.C. 20375

Attn: Code 1000 - CAPT. E. E. Henifin
1001 - Dr. A. Berman
4700 - Dr. T. Coffey (26 copies)
4701 - Mr. J. Brown
4740 - Dr. V. L. Granatstein (20 copies)
4740 - Dr. R. K. Parker (20 copies)
4740 - Dr. K. R. Chu
4740 - Dr. C. W. Roberson
4790 - Dr. P. Sprangle (100 copies)
4790 - Dr. C. M. Tang
4790 - Dr. M. Lampe
4790 - Dr. W. M. Manheimer
6603S- Dr. W. W. Zachary
6650 - Dr. L. Cohen
6656 - Dr. N. Seeman
6850 - Dr. L. R. Whicker
6805 - Dr. S. Y. Ahn
6875 - Dr. R. Wagner

On Site Contractors:
Code 4740 - Dr. L. Barnett (B-K Dynamics)
4740 - Dr. D. Dialetis (SAI)
4740 - Dr. Y. Y. Lau (SAI)
4790 - Dr. A. T. Drobot (SAI)
4790 - Dr. J. Vomvoridis (JAYCOR)
4790 - Dr. H. Freund (SAI)

* Every name listed on distribution gets one copy except for those where extra copies are noted.

Dr. Tony Armstrong
SAI, Inc.
P. O. Box 2351
La Jolla, CA 92038

Dr. Robert Behringer
ONR
1030 E. Green
Pasadena, CA 91106

Dr. G. Bekefi (5 copies)
Massachusetts Institute of Technology
Bldg. 26
Cambridge, MA 02139

Dr. Arden Bement (2 copies)
Deputy Under Secretary of Defense
for R&AT
Room 3E114, The Pentagon
Washington, D.C. 20301

MAJ Rettig P. Benedict, USAF
DARPA/STO
1400 Wilson Boulevard
Arlington, VA 22209

Dr. T. Berlincourt
Code 420
Office of Naval Research
Arlington, VA 22217

Dr. I. B. Bernstein (2 copies)
Yale University
Mason Laboratory
400 Temple Street
New Haven, CT 06520

Dr. Charles Brau (2 copies)
Applied Photochemistry Division
Los Alamos National Scientic
Laboratory
P. O. Box 1663, M.S. - 817
Los Alamos, NM 87545

Dr. R. Briggs (L-71)
Lawrence Livermore National Lab.
P. O. Box 808
Livermore, CA 94550

Dr. Fred Burskirk
Physics Department
Naval Postgraduate School
Monterey, CA 93940

Dr. K. J. Button
Massachusetts Institute of Technology
Francis Bitter National Magnet Lab.
Cambridge, MA 02139

Dr. Gregory Canavan
Director, Office of Inertial Fusion
U. S. Department of Energy
M.S. C404
Washington, D.C. 20545

Prof. C. D. Cantrell
Center for Quantum Electronics
& Applications
The University of Texas at Dallas
P. O. Box 688
Richardson, TX 75080

Dr. Maria Caponi
TRW, Building R-1, Room 1070
One Space Park
Redondo Beach, CA 90278

Dr. J. Cary
Los Alamos National Scienific
Laboratory
MS 608
Los Alamos, NM 87545

Dr. Weng Chow
Optical Sciences Center
University of Arizona
Tucson, AZ 85721

Dr. Peter Clark
TRW, Building R-1, Room 1096
One Space Park
Redondo Beach, CA 90278

Dr. Robert Clark
P. O. Box 1925
Washington, D.C. 20013

Dr. William Colson
Quantum Institute
Univ. of California at Santa Barbara
Santa Barbara, CA 93106

Dr. William Condell
Code 421
Office of Naval Research
Arlington, VA 22217

Dr. Richard Cooper
Los Alamos National Scientific Laboratory
P. O. Box 1663
Los Alamos, NM 87545

Cmdr. Robert Cronin
NFOIO Detachment, Suitland
4301 Suitland Road
Washington, D.C. 20390

Dr. R. Davidson (5 copies)
Plasma Fusion Center
Massachusetts Institute of Technology
Cambridge, MA 02139

Dr. John Dawson (2 copies)
Physics Department
University of California
Los Angeles, CA 90024

Dr. David Deacon
Physics Department
Stanford University
Stanford, CA 94305

Defense Technical Information Center (12 copies)
Cameron Station
5010 Duke Street
Alexandria, VA 22313

Dr. Francesco De Martini
Instituto de Fiscia
G. Marconi" Univ.
Piazzo delle Science, 5
ROMA00185 ITALY

Prof. P. Diament
Columbia University
Dept. of Electrical Engineering
New York, NY 10027

Prof. J. J. Doucet (5 copies)
Ecole Polytechnique
91128 Palaiseau
Paris, France

Dr. John Elgin (2 copies)
Imperial College
Dept. of Physics (Optics)
London SWF, England

Dr. Luis R. Elias (2 copies)
Quantum Institute
University of California
Santa Barbara, CA 93106

Dr. David D. Elliott
SRI International
33 Ravenswood Avenue
Menlo Park, CA 94025

Dr. Jim Elliot (2 copies)
X-Division, M.S. 531
Los Alamos National Scientific Laboratory
Los Alamos, NM 87545

Director (2 copies)
National Security Agency
Fort Meade, MD 20755
ATTN: Mr. Richard Foss, A42

Dr. Robert Fossum, Director
DARPA
1400 Wilson Boulevard
Arlington, VA 22209 (2 copies)

Dr. Edward A. Frieman
Director, Office of Energy Research
U. S. Department of Energy
M.S. 6E084
Washington, D.C. 20585

Dr. George Gamota (3 copies)
OUSDRE (R&AT)
Room 3D1067, The Pentagon
Washington, D.C. 20301

Dr. Richard L. Garwin
IBM, T. J. Watson Research Center
P. O. Box 218
Yorktown Heights, NY 10598

Dr. Edward T. Gerry, President
W. J. Schafer Associates, Inc.
1901 N. Fort Myer Drive
Arlington, VA 22209

Dr. Avraham Gover
Tel Aviv University
Fac. of Engineering
Tel Aviv, ISRAEL

Mr. Donald L. Haas, Director
DARPA/STO
1400 Wilson Boulevard
Arlington, VA 22209

Dr. P. Hammerling
La Jolla Institute
P. O. Box 1434
La Jolla, CA 92038

Director
National Security Agency
Fort Meade, MD 20755
ATTN: Mr. Thomas Handel, A243

Dr. William Happer
560 Riverside Drive
New York City, NY 10027

Dr. Robert J. Hermann
Assistant Secretary of the
Air Force (RD&L)
Room 4E856, The Pentagon
Washington, D.C. 20330

Dr. Rod Hiddleston
KMS Fusion
Ann Arbor, MI 48106

Dr. J. L. Hirshfield (2 copies)
Yale University
Mason Laboratory
400 Temple Street
New Haven, CT 06520

Dr. R. Hofland
Aerospace Corp.
P. O. Box 92957
Los Angeles, CA 90009

Dr. Fred Hopf
University of Arizona
Tucson, AZ 85721

Dr. Benjamin Huberman
Associate Director, OSTP
Room 476, Old Executive Office Bldg.
Washington, D.C. 20506

Dr. S. F. Jacobs
Optical Sciences Center
University of Arizona
Tucson, AZ 85721

Mr. Eugene Kopf
Principal Deputy Assistant
Secretary of the Air Force (RD&L)
Room 4E964, The Pentagon
Washington, D.C. 20330

Prof. N. M Kroll
La Jolla Institutes
P. O. Box 1434
La Jolla, CA 92038

Dr. Tom Kuper
Optical Sciences Center
University of Arizona
Tucson, AZ 85721

Dr. Thomas Kwan
Los Alamos National Scientific
Laboratory
MS608
Los Alamos, NM 87545

Dr. Willis Lamb
Optical Sciences Center
University of Arizona
Tucson, AZ 85721

Mr. Mike Lavan
BMDATC-O
ATTN: ATC-O
P. O. Box 1500
Huntsville, AL 35807

Dr. John D. Lawson (2 copies)
Rutherford High Energy Lab.
Chilton
Didcot, Oxon OX11 OOX
ENGLAND

Mr. Ray Leadabrand
SRI International
333 Ravenswood Avenue
Menlo Park, CA 94025

Mr. Barry Leven
NISC/Code 20
4301 Suitland Road
Washington, D.C. 20390

Dr. Donald M. LeVine (3 copies)
SRI International
1611 N. Kent Street
Arlington, VA 22209

Dr. Anthony T. Lin
University of California
Los Angeles, CA 90024

Director (2 copies)
National Security Agency
Fort Meade, MD 20755
ATTN: Mr. Robert Madden, R/SA

Dr. John Madey
Physics Department
Stanford University
Stanford, CA 94305

Dr. Joseph Mangano
DARPA
1400 Wilson Boulevard
Arlington, VA 22209

Dr. S. A. Mani
W. J. Schafer Associates, Inc.
10 Lakeside Office Park
Wakefield, MA 01880

Dr. Mike Mann
Hughes Aircraft Co.
Laser Systems Division
Culver City, CA 90230

Dr. T. C. Marshall
Applied Physics Department
Columbia University
New York, NY 10027

Mr. John Meson
DARPA
1400 Wilson Boulevard
Arlington, VA 22209

Dr. Pierre Meystre
Projektgruppe fur Laserforschung
Max Planck Gesellschaft
Garching, MUNICH WEST GERMANY

Dr. Gerald T. Moore
Optical Sciences Center
University of Arizona
Tucson, Az 85721

Dr. Philip Morton
Stanford Linear Accelerator Center
P. O. Box 4349
Stanford, CA 94305

Dr. Jesper Munch
TRW
One Space Park
Redondo Beach, CA 90278

Dr. George Neil
TRW
One Space Park
Redondo Beach, CA 90278

Dr. Kelvin Neil
Lawrence Livermore National Lab.
Code L-321, P. O. Box 808
Livermore, CA 94550

Dr. Brian Newnam
MS 564
Los Alamos National Scientific
Laboratory
P. O. Box 1663
Los Alamos, NM 87545

Dr. Milton L. Noble (2 copies)
General Electric Company
G. E. Electric Park
Syracuse, NY 13201

Prof. E. Ott (2 copies)
University of Maryland
Dept. of Physics
College Park, MD 20742

Dr. Richard H. Pantell
Stanford University
Stanford, CA 94305

Dr. Claudio Parazzoli
Highes Aircraft Company
Building 6, MS/C-129
Centinela & Teale Streets
Culver City, CA 90230

Dr. Richard M. Patrick
AVCO Everett Research Lab., Inc.
2385 Revere Beach Parkway
Everett, MA 02149

Dr. Claudio Pellegrini
Brookhaven National Laboratory
Associated Universities, Inc.
Upton, L.I., NY 11973

The Honorable William Perry
Under Secretary of Defense (R&E)
Office of the Secretary of Defense
Room 3E1006, The Pentagon
Washington, D.C. 20301

Dr. Alan Pike
DARPA/STO
1400 Wilson Boulevard
Arlington, VA 22209

Dr. Hersch Pilloff
Code 421
Office of Naval Research
Arlington, VA 22217

Dr. Charles Planner
Rutherford High Energy Lab.
Chilton
Didcot, Oxon, OX11, 00X
ENGLAND

Dr. Michal Poole
Daresbury Nuclear Physics Lab.
Daresbury, Warrington
Cheshire WA4 4AD
ENGLAND

Dr. Don Prosnitz
Lawrence Livermore National Lab.
Livermore, CA 94550

Dr. D. A. Reilly
AVCO Everett Research Lab.
Everett, MA 02149

Dr. James P. Reilly
W. J. Schafer Associates, Inc.
10 Lakeside Office Park
Wakefield, MA 01880

Dr. A. Renieri
C.N.E.N.
Div. Nuove Attivita
Dentro di Frascatti
Frascatti, Rome
ITALY

Dr. Daniel N. Rogovin
SAI
P. O. Box 2351
La Jolla, CA 92038

Dr. Michael Rosenbluh
MIT - Magnet Laboratory
Cambridge, MA 02139

Dr. Marshall N. Rosenbluth
Institute for Advanced Study
Princeton, NJ 08540

Dr. Eugene Ruane (2 copies)
P. O. Box 1925
Washington, D.C. 20013

Dr. Antonio Sanchez
MIT/Lincoln Laboratory
Room B231
P. O. Box 73
Lexington, MA 02173

Dr. Aleksandr N. Sandalov
Department of Physics
Moscow University
MGU, Lenin Hills
Moscow, 117234, USSR

Prof. S. P. Schlesinger
Columbia University
Dept. of Electrical Engineering
New York, NY 10027

Dr. Howard Schlossberg
AFOSR
Bolling AFB
Washington, D.C. 20332

Dr. Stanley Schneider
Rotodyne Corporation
26628 Fond Du Lac Road
Palos Verdes Peninsula, CA 90274

Dr. Marlan O. Scully
Optical Science Center
University of Arizona
Tucson, AZ 85721

Dr. Steven Segel
KMS Fusion
3621 S. State Street
P. O. Box 1567
Ann Arbor, MI 48106

Dr. Robert Sepucha
DARPA/STO
1400 Wilson Boulevard
Arlington, VA 22209

Dr. A. M. Sessler
Lawrence Berkeley Laboratory
University of California
1 Cyclotron Road
Berkeley, CA 94720

Dr. Earl D. Shaw
Bell Labs
600 Mountain Avenue
Murray Hill, NJ 07974

Dr. Chan-Chin Shih
R&D Associates
P. O. Box 9695
Marina Del Rey, CA 92091

Dr. Jack Slater
Mathematical Sciences, NW
P. O. Box 1887
Bellevue, WA 98009

Dr. Kenneth Smith
Physical Dynamics, Inc.
P. O. Box 556
La Jolla, CA 92038

Mr. Todd Smith
Hansen Labs
Stanford University
Stanford, CA 94305

Dr. Joel A. Snow
Senior Technical Advisor
Office of Energy Research
U. S. Department of Energy, M.S. E084
Washington, D.C. 20585

Dr. Richard Spitzer
Stanford Linear Accelerator Center
P. O. Box 4347
Stanford, CA 94305

Mrs. Alma Spring
DARPA/Administration
1400 Wilson Boulevard
Arlington, VA 22209

DRI/MP Reports Area G037 (2 copies)
333 Ravenswood Avenue
Menlo Park, CA 94025
ATTN: D. Leitner

Dr. Abraham Szoke
Lawrence Livermore National Lab.
MS/L-470, P. O. Box 808
Livermore, CA 94550

Dr. Milan Tekula
AVCO Everett Research Lab.
2385 Revere Beach Parkway
Everett, MA 02149

Dr. John E. Walsh
Department of Physics
Dartmouth College
Hanover, NH 03755

Dr. Wasneski (2 copies)
Naval Air Systems Command
Department of the Navy
Washington, D.C. 20350

Ms. Bettie Wilcox
Lawrence Livermore National Lab.
ATTN: Tech. Info. Dept. L-3
P. O. Box 808
Livermore, CA 94550

Dr. A. Yariv
California Institute of Tech.
Pasadena, CA 91125